

RESEARCH ARTICLE

The sensitivity of the West African monsoon circulation to intraseasonal soil moisture feedbacks

Joshua Talib¹  | Christopher M. Taylor^{1,2}  | Cornelia Klein^{1,3}  |
Bethan L. Harris^{1,2}  | Seonaid R. Anderson¹  | Valiyaveetil S. Semeena¹ 

¹UK Centre for Ecology and Hydrology, Wallingford, UK

²National Centre for Earth Observation, Wallingford, UK

³Department of Atmospheric and Cryospheric Sciences, University of Innsbruck, Innsbruck, Austria

Correspondence

J. Talib, UK Centre for Ecology and Hydrology, Wallingford, OX10 8BB, UK.
Email: jostal@ceh.ac.uk

Funding information

Department for International Development, Grant/Award Numbers: NE/M020428/2, NE/S006087/1; Global Challenges Research Fund, Grant/Award Number: NE/P021077/1; Natural Environment Research Council, Grant/Award Number: NE/R016518/1

Abstract

Intraseasonal soil moisture variability has the potential to feed back onto the West Africa monsoon circulation through its influence on surface turbulent fluxes and planetary boundary-layer characteristics. Using satellite observations and an atmospheric reanalysis, we investigate intraseasonal soil moisture–atmosphere feedbacks triggered by large-scale dynamics within the West African monsoon. Surprisingly, even though the surface response across the Sahel to strong convection is short-lived (days) and precipitation accumulations are spatially and temporally heterogeneous, a coherent regional-scale surface response to intraseasonal variability is observed. This surface response then feeds back onto the West African monsoon circulation. For example, during a dry intraseasonal event, Sahelian surface soil moisture significantly decreases, which elevates surface temperatures by 1.5 °C and shifts the monsoon circulation southward by approximately 1.5° latitude. Also, during a wet event the surface moistens and cools which leads to a northward monsoon shift. Alongside a low-level wind response, the African Easterly Jet (AEJ) also responds to surface changes due to variations in the meridional temperature gradient. For example, an increased temperature gradient during a dry event intensifies and shifts the AEJ southward. The combined response of low-level monsoon westerlies and the AEJ impacts low-level shear and characteristics of strong convection. Elevated low-level shear during a dry event promotes an intensification of deep convection across southern West Africa. This study provides new insight into the sensitivity of the West African monsoon circulation to intraseasonal soil moisture feedbacks and encourages similar research in other regions. An improved understanding and model representation of soil moisture–atmosphere feedbacks has the potential to improve forecasts beyond daily time-scales and enhance early warning systems.

KEYWORDS

convection, intraseasonal variability, land surface, monsoon circulation, soil moisture–atmosphere feedbacks, West Africa

1 | INTRODUCTION

In regions with limited soil moisture and vegetation, the surface response to rainfall feeds back onto the atmosphere due to a strong sensitivity of surface turbulent fluxes. When potential evaporation exceeds precipitation, sensible heat is favoured over evapotranspiration as the surface dries and warms (Teuling *et al.*, 2006; Miralles *et al.*, 2012; Gallego-Elvira *et al.*, 2016), which can increase near-surface air temperatures and deepen the planetary boundary layer (Koster *et al.*, 2009; Miralles *et al.*, 2012; Berg *et al.*, 2014; Schwingshackl *et al.*, 2017). The atmospheric response to variations in soil moisture and the surface energy balance can affect the likelihood of deep convection (Findell and Eltahir, 2003; Taylor *et al.*, 2012; Bhowmick and Parker, 2018) and drive daytime circulations which are orientated by soil moisture gradients (Pielke, 2001; Taylor *et al.*, 2007; Taylor, 2015; Barton *et al.*, 2021). Previous studies have shown the influence of soil moisture–atmosphere feedbacks across West Africa on daily mesoscale precipitation variability (Taylor *et al.*, 2012; Klein and Taylor, 2020). Meanwhile, the impact of intraseasonal soil moisture variability on the West African monsoon has only been investigated for the ‘Sahel’ mode (Sultan and Janicot, 2003; Taylor, 2008; Lavender *et al.*, 2010), even though intraseasonal surface fluctuations have been shown to affect regional circulations in other tropical regions (Saha *et al.*, 2012; Unnikrishnan *et al.*, 2017; Chug and Dominguez, 2019).

Tropical rainfall exhibits substantial intraseasonal variability (Pegion and Kirtman, 2008) and, on a global scale, is predominately controlled by the Madden–Julian Oscillation (MJO; Madden and Julian, 1994). Several studies show an influence of land–atmosphere feedbacks on intraseasonal variations of tropical rainfall and monsoon circulations. The majority of this research has focused on 30- to 60-day variability of the South Asian monsoon, which is characterised by strong convection that forms north of the Equator and propagates northward (Sikka and Gadgil, 1980; Webster, 1983; Gadgil and Asha, 1992; Annamalai and Slingo, 2001). Model simulations show that the intensity of 30- to 60-day variations of the South Asian monsoon is sensitive to the representation of surface hydrology (Webster, 1983; Srinivasan *et al.*, 1993; Ferranti *et al.*, 1999; Saha *et al.*, 2012; Unnikrishnan *et al.*, 2017). Ahead of strong convection associated with a wet intraseasonal event, dry soils increase anomalies in sensible heat and atmospheric instability which lead to an intensification of deep convection. As a result, prescribing fixed soil moisture reduces the intensity of the 30- to 60-day variability (Ferranti *et al.*, 1999; Saha *et al.*, 2012; Unnikrishnan *et al.*, 2017) and, in cases where only a single surface layer is represented and soil moisture cannot be transferred to

greater depths, intraseasonal variability of the South Asian monsoon is removed altogether (Webster, 1983; Srinivasan *et al.*, 1993).

A dynamical atmospheric response to monthly surface fluctuations is also observed across the La Plata basin in southeastern South America (Chug and Dominguez, 2019). Monthly variability across the basin is associated with a dipole in vegetation changes. Increased vegetation across the northeast promotes low-level cooling and a high pressure tendency, whilst decreased vegetation across the southwest leads to low-level warming and a low pressure tendency. The dynamical atmospheric response to surface-induced temperature changes promotes northerly winds which enhance moisture convergence and rainfall across central and southern regions of the basin (Chug and Dominguez, 2019). The impact of intraseasonal land–atmosphere feedbacks on the atmospheric circulation has predominately been explored across India and South America, as these land regions exhibit the largest intraseasonal rainfall variations (Waliser, 2006). Whilst intraseasonal rainfall variability is smaller across West Africa (Waliser, 2006), land–atmosphere feedbacks on shorter time-scales play a key role in determining characteristics of the West African monsoon and deep convection (i.e., Taylor *et al.*, 2011; 2012; Klein and Taylor, 2020). In light of this, we investigate the influence of intraseasonal soil moisture–atmosphere feedbacks on characteristics of the West African monsoon.

The West African monsoon circulation, which is responsible for the majority of annual precipitation across West Africa (Sultan and Janicot, 2000; 2003), is driven by a strong meridional temperature gradient between the Sahara and Gulf of Guinea. Figure 1 shows the climatological precipitation, low-level atmospheric temperature, and horizontal wind when the West African monsoon is active during June to September. Across the Sahara, strong solar surface heating promotes a heat low circulation which drives southwesterly monsoon winds, which transport moisture from the Gulf of Guinea, and deflects dry northeasterlies from the Sahara (Figure 1b; Lafore *et al.*, 2011). The latitude where moist southwesterlies meet dry northeasterlies is often called the “intertropical discontinuity” (ITD; cf. Figure 1b). Above the planetary boundary layer, the low-level meridional temperature gradient drives the African Easterly Jet (AEJ; cf. Figure 1a), which is observed at approximately 600 hPa with a peak wind speed between 10 and 20 m s^{−1} (Cook, 1999; Thorncroft and Hodges, 2001). The monsoon rainbelt sits on the southern flank of the AEJ and within a region of low-level southwesterly monsoon winds (Figure 1), thus the rainbelt is situated in an area with strong vertical wind shear. Strong convection is favoured in regions with substantial low-tropospheric shear and moisture (Rowell and

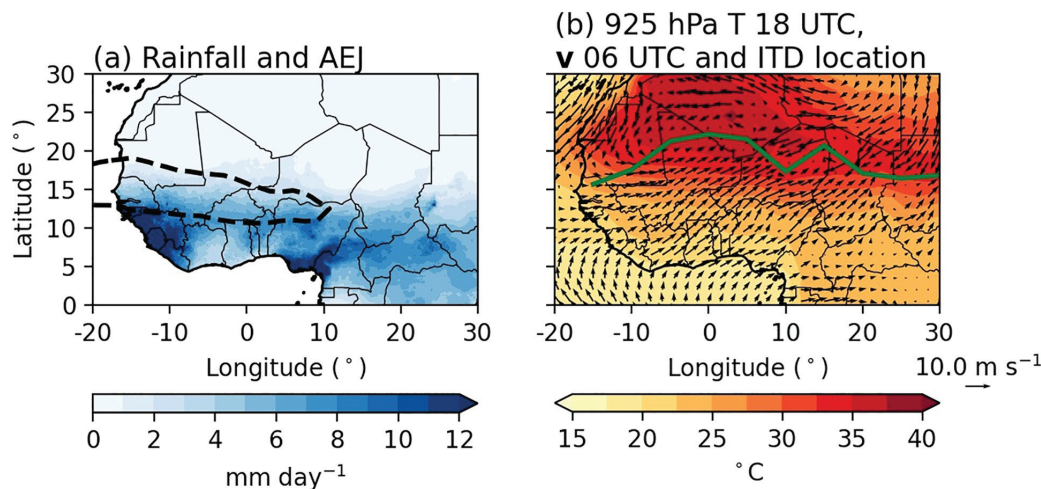


FIGURE 1 June to September climatology between 1981 and 2020 during the active West African monsoon season. (a) CHIRPS precipitation (shading, $\text{mm}\cdot\text{day}^{-1}$) and a $-10\text{ m}\cdot\text{s}^{-1}$ dashed black contour of the 600 hPa zonal wind denoting the AEJ. (b) 1800 UTC 925 hPa air temperature (shading, $^{\circ}\text{C}$) and 0600 UTC 925 hPa horizontal wind (arrows, $\text{m}\cdot\text{s}^{-1}$). The green line in (b) denotes the approximate location of the intertropical discontinuity

Milford, 1993; Hodges and Thorncroft, 1997; Nicholls and Mohr, 2010), with deep convection being intense when the AEJ is strong (Mohr and Thorncroft, 2006) or when the ITD shifts southwards and low-level convergence is enhanced (Vizy and Cook, 2018; Klein and Taylor, 2020). There is also a substantial diurnal cycle of the low-level monsoon winds that transport moisture inland. During the day, solar-driven surface warming drives strong surface turbulent fluxes that deepen the convective boundary layer and prohibit a low-level wind response to the meridional temperature gradient. Instead, winds and the advection of moisture peak after sunset once turbulent fluxes reduce and a stable boundary layer is formed (Rácz and Smith, 1999; Parker *et al.*, 2005).

Intraseasonal variability of the West African monsoon is typically categorised into variations shorter or longer than 20 days (Janicot and Sultan, 2001; Maloney and Shaman, 2008). There are two leading modes of intraseasonal variability shorter than 20 days (Janicot *et al.*, 2011): the Quasi-Biweekly Zonal Dipole (QBZD; Mounier *et al.*, 2008) and the ‘Sahel’ mode (Sultan and Janicot, 2003; Janicot *et al.*, 2011). The QBZD is a quasi-stationary zonal dipole of convection, driven by a Kelvin wave-like disturbance, with approximately 5.5 strong and weak events every boreal summer (Mounier *et al.*, 2008). Its characteristics are similar to a near-equatorial Walker-type circulation with positive convective anomalies over West Africa occurring simultaneously with negative convective anomalies over the equatorial West Atlantic Ocean (Mounier *et al.*, 2008). Meanwhile, the Sahel mode initiates over eastern equatorial Africa, propagates northwards to 15°N , and then travels westwards into the Atlantic Ocean

(Janicot *et al.*, 2011). The average time period for the Sahel mode is approximately 15 days and has been shown to be partly driven by equatorial Rossby waves (Janicot *et al.*, 2010) and intraseasonal variability of the extratropical circulation (Roehrig *et al.*, 2011). Taylor (2008) showed that the westward propagation of the Sahel mode is partly controlled by surface moisture anomalies feeding back onto the regional circulation. Surface moistening during enhanced rainfall decreases boundary-layer temperatures and promotes an anticyclonic circulation, which intensifies monsoon westerlies to the west of strong convection and encourages the westward propagation of rainfall anomalies. Modelling experiments with and without prognostic soil moisture illustrate that moisture anomalies enhance and organise the Sahel mode (Lavender *et al.*, 2010). However, 15-day rainfall variability associated with westward propagating rainfall anomalies are still present when removing soil moisture variations, highlighting the importance of convectively coupled equatorial waves and associated radiation–atmosphere interactions (Mounier *et al.*, 2008). Whilst soil moisture–atmosphere feedbacks influence characteristics of the Sahel mode, surface hydrology appears to play a more passive role in controlling variability induced by the QBZD, which is mainly controlled by radiation–atmosphere interactions (Mounier *et al.*, 2008; Janicot *et al.*, 2011). Minimal convection increases surface net-downward short-wave radiation and temperature which leads to a surface pressure reduction and an intensification of low-level monsoon westerlies and convective activity. Whilst previous studies have explored the influence of soil moisture–atmosphere feedbacks on characteristics of intraseasonal variability shorter

than 20 days, it still remains to be understood whether the surface response to variability greater than 20 days feeds back to the monsoon circulation.

Two mechanisms have been proposed for intraseasonal variability of the West African monsoon greater than 20 days. The first is a remote response to MJO-induced convective anomalies across the equatorial West Pacific warm pool. These anomalies promote dry equatorial westward-propagating Rossby waves and eastward-propagating Kelvin waves that reach West Africa approximately 20 days after initiation (Matthews, 2004; Lavender and Matthews, 2009). Cool mid-tropospheric temperatures associated with these equatorial waves favour deep convection. Along with Matthews (2004) and Lavender and Matthews (2009) highlighting a remote atmospheric response to MJO-induced convective anomalies across the West Pacific, previous studies also show that the MJO influences convection across West Africa (Annamalai and Slingo, 2001; Maloney and Shaman, 2008; Berhane *et al.*, 2015; Schlueter *et al.*, 2019b), changes the frequency of extreme precipitation events (Sossa *et al.*, 2017), and impacts the development of African easterly waves (Ventrice *et al.*, 2011). The second mechanism proposed for intraseasonal variability greater than 20 days is a response to the northward propagation of a meridional dipole in anomalous convection across the Indian Ocean and continent (Janicot *et al.*, 2009). Enhanced convection, and associated low-level negative geopotential anomalies, is observed across northwest India 20 days before intense convection across West Africa. These low-level negative geopotential anomalies extend westward, eventually become isolated over West Africa, and promote low-level monsoon westerlies which favour deep convection (Janicot *et al.*, 2009). It is likely that both mechanisms proposed by Matthews (2004) and Janicot *et al.* (2009) play a role in intraseasonal variability of the West African monsoon.

In this study we investigate whether soil moisture–atmosphere feedbacks across the Sahel, driven by intraseasonal variability of the West African monsoon greater than 20 days, influence the large-scale

monsoon circulation and characteristics of deep convection. To do this, we first assess the surface response across West Africa to intraseasonal events. We then investigate whether the surface response drives a soil moisture–atmosphere feedback that affects the dynamics of the West African monsoon circulation and characteristics of deep convection. Section 2 outlines the observations and reanalysis utilised in this study (Section 2.1), along with the technique used to diagnose intraseasonal variability (Section 2.2). The results section of this study is separated into two parts with section 3 discussing the surface response to intraseasonal rainfall fluctuations, and section 4 exploring the impacts of soil moisture–atmosphere feedbacks on the dynamics of the West African monsoon circulation (Section 4.1) and characteristics of deep convection (Section 4.2). Finally, Sections 5 and 6 close the paper with the discussion and conclusions respectively.

2 | METHODOLOGY

2.1 | Data

In this study multiple observational products are used to understand intraseasonal land–atmosphere feedbacks across West Africa. Table 1 provides an overview of all datasets utilised. To diagnose 20- to 200-day variability of convective activity during the West African monsoon, we use daily-mean outgoing long-wave radiation (OLR) satellite observations from the National Oceanic and Atmospheric Administration (Liebmann and Smith, 1996). These OLR observations were retrieved between June to September (JJAS) 1979 to 2020 at a 2.5° latitude by 2.5° longitude resolution. To investigate precipitation variations associated with intraseasonal OLR variability, we use the Climate Hazards Group InfraRed Precipitation with Stations (CHIRPS) dataset, which combines satellite-derived infrared measurements with gauge-based rainfall totals (Funk *et al.*, 2015). As CHIRPS data are

TABLE 1 Observational and reanalysis products used in this study

Variable	Data source	Time span	Reference
Outgoing long-wave radiation	NOAA	1979 to 2020	Liebmann and Smith (1996)
Precipitation	CHIRPS	1981 to 2020	Funk <i>et al.</i> (2015)
Surface soil moisture	ESA CCI	1981 to 2020	Dorigo <i>et al.</i> (2017)
Land surface temperature	SEVIRI MSG	2004 to 2020	Sobrino and Romaguera (2004)
Vegetation optical depth	VODCA	2000 to 2018	Moesinger <i>et al.</i> (2020)
Atmospheric conditions	ERA5	1981 to 2020	Hersbach <i>et al.</i> (2019)
Thermal infrared brightness temperature	SEVIRI Meteosat satellites	1982 to 2020	

available from 1981, we investigate intraseasonal soil moisture–atmosphere feedbacks from 1981 to 2020.

Three satellite-derived observational datasets are used to investigate the surface response to intraseasonal variability. To analyse changes in surface soil moisture, we use satellite retrievals from the European Space Agency Climate Change Initiative (ESA CCI) combined soil moisture product v06.1 (Dorigo *et al.*, 2017; Gruber *et al.*, 2017, 2019; van der Schalie *et al.*, 2020). We use retrievals from 1981 to 2020. The combined soil moisture product utilises four active and ten passive microwave-based instruments alongside a global land data assimilation system (GLDAS; Rodell *et al.*, 2004) to obtain a consistent climatology (Gruber *et al.*, 2019). There is no common definition for the soil moisture depth examined by microwave-based instruments (Dorigo *et al.*, 2017); however, it is generally assumed to be in the range of 2 to 5 cm (Ulaby *et al.*, 1982).

In addition to surface soil moisture measurements, we also use land surface temperature (LST) observations as a direct measurement of changes in the surface energy balance. Across West Africa, LST anomalies indicate surface variability driven by soil moisture and a changed partitioning between surface sensible and latent heat fluxes. Daytime-mean (0700–1700 UTC) LST anomalies observed between 2004 and 2020 are computed from 15-min infrared observations at a 3 km resolution obtained from Spinning Enhanced Visible and Infrared Imager (SEVIRI) on Meteosat Second Generation (MSG; Sobrino and Romaguera, 2004). Whilst the time span of LST observations is shorter than soil moisture retrievals (Table 1), we capture the LST response during a sufficient number of intraseasonal events to understand changes in the surface energy balance. LST data are only available for cloud-free pixels, and although a cloud-mask is routinely applied to SEVIRI LSTs operationally, our initial analysis indicated that partially cloudy pixels are often missed, which can have a substantial cooling effect on temperature anomalies. In this study we therefore developed a new cloud-masking process on top of the operational mask provided. Firstly, as incorrect pixel identification was often found near the edges of clouds, any pixels identified as cloud in the previous three 15-min images, or in the next image, were removed. We then analyse the difference between consecutive LST observations, as intermittent cloud introduces high-frequency noise into the diurnal cycle of LST. Specifically, changes in LST between two images 15 min apart were compared with the climatological distribution of temperature changes (Hclim). Hclim was calculated for each time of day and pixel using LST data from 2004 to 2015 and combining data over a 31-day period centred on each date. Pixels with a temperature change greater or lower than two standard deviations of Hclim were removed. Pixels with fewer than fifty points

contributing to Hclim were also removed. In this study we subtract the 30-day rolling mean to compute anomalous LST, and only show daytime (0700 to 1700 UTC) anomalies averaged onto a 0.25° grid with the climatological daytime anomaly subtracted from each pixel. Note that, whilst the availability of LST images every 15 min produces an improved estimate of daytime mean conditions, it requires substantial volumes of data. For this reason we process only a West African domain extending to 20°N.

We also exploit vegetation optical depth (VOD) observations from the vegetation optical depth climate archive (VODCA) dataset (Moesinger *et al.*, 2020) as we expect intraseasonal variability to lead to vegetation cover fluctuations that cause surface flux anomalies which are more persistent than anomalies due to surface soil moisture variations. VOD is derived from satellite-based measurements of microwave radiation, as vegetation attenuates the amount of microwave radiation emitted or reflected by the surface. The level of attenuation depends on multiple factors including vegetation density, vegetation type, and water content. In this study, VOD is used as a metric for vegetation biomass. We use VOD observations retrieved between 2000 and 2018 in the X-band (≈ 10.7 GHz), and exclude data flagged with processing irregularities. We also process VOD data to remove spurious observations and VOD fluctuations that are caused by changes in surface water. Similar to errors observed in SEVIRI LSTs, unprocessed VOD data include observations that are substantially different from previous and subsequent daily measurements. To remove these spurious observations, we produced a monthly climatology of VOD changes between two consecutive valid observations at each grid point. We then removed all daily observations where VOD changes are greater than two standard deviations from the climatology both before and after the daily observation. As well as removing spurious observations, we have also removed 7-day periods where VOD changes are most likely due to changes in surface water. Bousquet *et al.* (2021) highlights that inundation leads to an apparent decrease in VOD. To remove the impact of inundation on VOD measurements, we use daily surface water observations, from the surface water microwave product series (SWAMPS) v3.2 dataset (Schroeder *et al.*, 2015), and ESA CCI soil moisture. We remove 7-day periods of VOD observations where the linear trend in VOD is smaller than the 15th percentile and the linear trend in surface soil moisture is greater than the 85th percentile. We have also removed VOD observations after the 7-day period where anomalous surface water and VOD is dissipating from the initial inundation event. The end of this period is defined where the 25-day rolling window of 7-day means in VOD and surface water is no longer significantly correlated ($p < 0.1$).

To investigate the atmospheric response to soil moisture–atmosphere feedbacks, we use European Centre for Medium-range Weather Forecasts (ECMWF) reanalysis v5 (ERA5; C3S, 2017; Hersbach *et al.*, 2019). We analyse data from 1981 to 2020 at a three-hourly 1.5° resolution on 22 pressure levels, 1,000 to 50 hPa in increments of 50 hPa with the addition of 975 and 925 hPa. ERA5, computed using 4D-Var data assimilation and cycle 41r2 of the Integrated Forecasting System (IFS), provides a detailed record of the global atmosphere, land surface and ocean waves (Hersbach *et al.*, 2018, 2019). ERA5 surface conditions are formulated using the hydrology-tiled ECMWF scheme for surface exchanges over land (HTESSEL) model (Balsamo *et al.*, 2015) which is forced using assimilated near-surface meteorological observations and soil moisture data from the Advanced Scatterometer (ASCAT; Wagner *et al.*, 2013; ECMWF, 2016). The use of ASCAT measurements to assimilate soil moisture will most likely improve the representation of planetary boundary-layer dynamics associated with intraseasonal soil moisture–atmosphere feedbacks. To minimise the impact of sampling across different months, we analyse all variables mentioned so far, except for LST and OLR, using anomalies relative to monthly climatologies and, where applicable, relative to hourly climatologies of the respective month.

To investigate the sensitivity of deep convection to intraseasonal soil moisture–atmosphere feedbacks, we analyse two metrics computed from thermal infrared brightness temperatures ($10.8\ \mu\text{m}$, channel 9) from Meteosat First and Second Generation satellites. Using both series of satellites generates a record of cloud-top temperatures from 1982 to 2020. The first metric is the percentage area covered by cloud-top temperatures $< -40^\circ\text{C}$ on a 1° latitude by 1° longitude grid. The second metric is the average minimum cloud-top temperature of each convective system when identifying storms through applying a two-dimensional wavelet scale decomposition to the cloud-top temperature field, following work by Klein *et al.* (2018). In this study, we define a convective event as contiguous cloud cover with a minimum area of $350\ \text{km}^2$ at a temperature $\leq -40^\circ\text{C}$. Meteosat First Generation satellites provided observations every 30 min at a resolution of approximately 4.5 km at the Equator. Meanwhile, MSG satellites provide observations at a higher spatial (approximately 3 km) and temporal (15 min) resolution. To minimise the impact of resolution between the two satellite series, we degrade images to a resolution of approximately 9 km. We also present cloud data only at 1800 UTC, as this is the time of day when the average vertical extent of deep convective systems across the Sahel is maximised (Futyan and Del Genio, 2007).

2.2 | Diagnosing intraseasonal variability

In this study we follow the same technique as Matthews (2004) and Janicot *et al.* (2009) to diagnose intraseasonal variability greater than 20 days across West Africa (-10 to 20°N , -40 to 40°E ; region shown in Figure 2a). Seasonal variations are removed from OLR observations using discrete Fourier transform before passing anomalies through a 241-weight 20- to 200-day bandpass Lanczos filter (Duchon, 1979). Intraseasonal variability is then diagnosed by computing the EOFs associated with 20- to 200-day filtered OLR anomalies. The leading eigenvector (EOF1) accounts for 15.8% of the variance whilst the second and third eigenvectors account for 8.1 and 7.0% of the variance respectively (not shown). Whilst the first and second eigenvectors are well separated from the subsequent eigenvectors, the remaining eigenvectors are degenerate and are not well separated based on the sampling noise criteria from North *et al.* (1982). Therefore we investigate soil moisture–atmosphere feedbacks associated only with EOF1. Figure 2a shows EOF1 with negative OLR anomalies denoting enhanced convection. As previously shown by Matthews (2004), negative OLR anomalies are found across two regions: one zonal band between 10 and 15°N and another southeastward-orientated band over West and Central Africa.

Intraseasonal soil moisture–atmosphere feedbacks are investigated using time-lagged composites centred on maxima and minima of the first principal component time series (PC1; Figure 2c). As maxima and minima in PC1 are associated with increased and decreased precipitation respectively, the corresponding composites are referred to as “wet event” and “dry event” composites. For our analysis we only consider maxima and minima in PC1 that have a magnitude greater than one standard deviation of the PC1 time series for a minimum of three days. Whilst the leading EOF is calculated using OLR data from 1979 to 2020, we focus on intraseasonal events from 1981 due to the time span of CHIRPS data. When considering the full JJAS period we observe 73 wet and 61 dry intraseasonal events. However, whilst wet events occur throughout the monsoon season, a substantial fraction of dry events, approximately 33%, occur within 10 days of the monsoon onset (not shown). This agrees with Sultan and Janicot (2000), who identified a precipitation reduction across West Africa before monsoon onset. As atmospheric characteristics dramatically change during the onset of the West African monsoon (Sultan and Janicot, 2000; 2003), we only retain maxima and minima in PC1 that occur 10 days after the monsoon onset. To define the monsoon onset we use CHIRPS data averaged onto a 2.5° latitude by

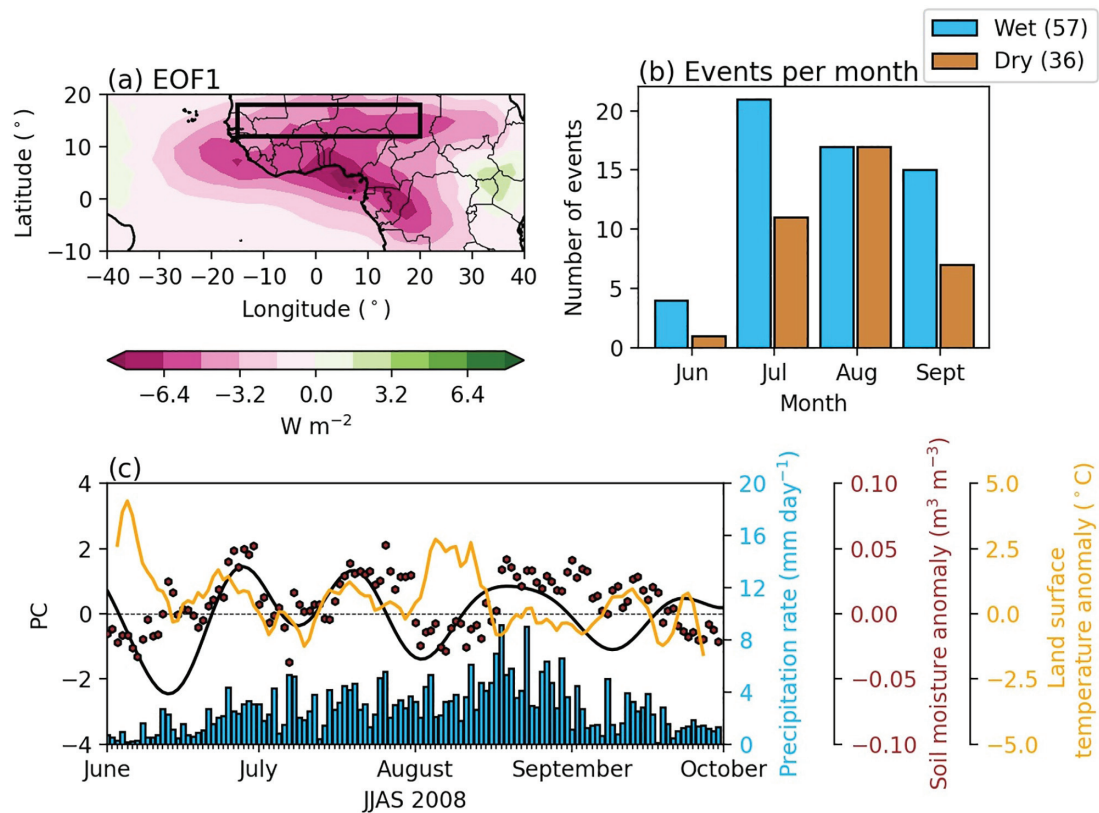


FIGURE 2 (a) EOF1 of 20- to 200-day filtered OLR anomalies over tropical Africa (-10 to $20^{\circ}N$, -40 to $40^{\circ}E$) for JJAS 1979 to 2020 (shading, $W \cdot m^{-2}$). The black rectangle denotes the Sahel region (12 – $18^{\circ}N$, -15 to $20^{\circ}E$). (b) The number of wet (blue) and dry (brown) post-monsoon onset intraseasonal events between 1981 and 2020 centred in each month of JJAS. The total number of wet and dry events is labelled in the legend. (c) OLR-based PC1 time series (black solid line) for JJAS 2008 alongside Sahelian-mean, regional-mean precipitation (blue bars, $mm \cdot day^{-1}$). (c) also shows anomalies of soil moisture (brown dots, $m^3 \cdot m^{-3}$) and daytime LST (orange line, $^{\circ}C$). For anomalous LST, a 5-day rolling mean is performed

2.5° longitude grid and the same methodology as Sultan and Janicot (2003). The mean date computed for the West African monsoon onset for the period of 1981 to 2020 is 21 June with a standard deviation of 9 days. To exclude onset-related events, we consider the onset date of each individual year and remove any events that occur before the onset date or within 10 days after. This subsetting of events results in 57 wet and 36 dry events that occur during the active monsoon period; these events will be used in all the following analyses. Figure 2b shows the number of dry and wet events observed in each month after filtering. Our criteria for selecting events means that we only study intraseasonal soil moisture–atmosphere feedbacks once the West African monsoon is fully developed.

To consider the potential large-scale drivers of the initiation and intensification of individual intraseasonal events, we evaluate the phase and intensity of the MJO during the progression of each event. The initiation and intensification of a substantial fraction of events across West Africa is associated with the MJO (not shown), in line with previous studies highlighting the influence of

the MJO on intraseasonal variability across West Africa (Matthews, 2004; Maloney and Shaman, 2008; Lavender and Matthews, 2009; Schlueter *et al.*, 2019a; 2019b). The MJO is active for approximately 54% and 62% of wet and dry intraseasonal events respectively. It should also be noted that the initiation and intensification of an intraseasonal event is favoured during certain phases of the MJO, in line with MJO-induced convective anomalies (Sossa *et al.*, 2017). The intensification of approximately 46% of wet events occurs during MJO phases 1 or 2, whilst the MJO is in phases 5 or 6 during the intensification of 42% of dry events. Whilst the MJO plays a substantial role in intraseasonal variability across West Africa, approximately 42% of intraseasonal events are associated with neutral MJO conditions and hence linked to other drivers. For example, Schlueter *et al.* (2019b) illustrate that intraseasonal variability is partly driven by equatorial Rossby waves. To fully understand the response of soil moisture–atmosphere feedbacks to intraseasonal variability, we have kept all events in each composite regardless of the MJO phase or intensity.

3 | SURFACE RESPONSE TO INTRASEASONAL VARIABILITY

To determine whether the surface feeds back onto the atmosphere during an intraseasonal dry or wet event, we first investigate the surface response to intraseasonal variability. Figure 2c shows a time series of anomalous Sahelian-mean soil moisture and LST during JJAS 2008 along with the PC1 time series and Sahelian-averaged precipitation. A 5-day running mean is applied to anomalous LST as cloud cover variations affect the parts of the Sahel which are observed on a given day. Focusing on a single boreal summer season illustrates that, even though precipitation across the Sahel varies substantially on time-scales smaller than 20 days (Janicot *et al.*, 2011), coherent intraseasonal fluctuations in anomalous soil moisture and LST occur. For example, LST anomalies which are out of phase with anomalous soil moisture vary by approximately 2 to 3°C on intraseasonal time-scales. We also observe a strong relationship between the PC1 time series and Sahelian surface characteristics. For example, at the start of August 2008, negative PC1 and low Sahelian precipitation is associated with surface drying and warming. On the other hand, positive PC1

values during late June and late August are associated with surface moistening and cooling. It is evident from observations in 2008 alone that intraseasonal rainfall variability impacts surface conditions, and, as LST anomalies are computed during clear-sky periods (Section 2.1), intraseasonal LST fluctuations across the Sahel are driven by changes in surface moisture rather than insolation.

To quantify the surface response to intraseasonal variability, we produce a composite of dry and wet intraseasonal events defined by the PC1 time series (Section 2.2). Figure 3 shows the Sahelian-mean anomalous OLR, precipitation, surface soil moisture, LST, and VOD during intraseasonal events which are defined using the whole West African domain (Figure 2a). During wet intraseasonal events the surface moistens and cools across the Sahel (Figure 3c), whilst during dry events, the surface dries and warms (Figure 3d). To further highlight the Sahelian surface response to intraseasonal variability, we compute the linear regression in surface characteristics between days -10 and +6 (inclusive) from the maximum and minimum in PC1 (dashed lines in Figure 3c,d). These days are chosen as they roughly correspond to the beginning and end of precipitation anomalies. For the rest of this study, we refer to these linear regressions as the wet

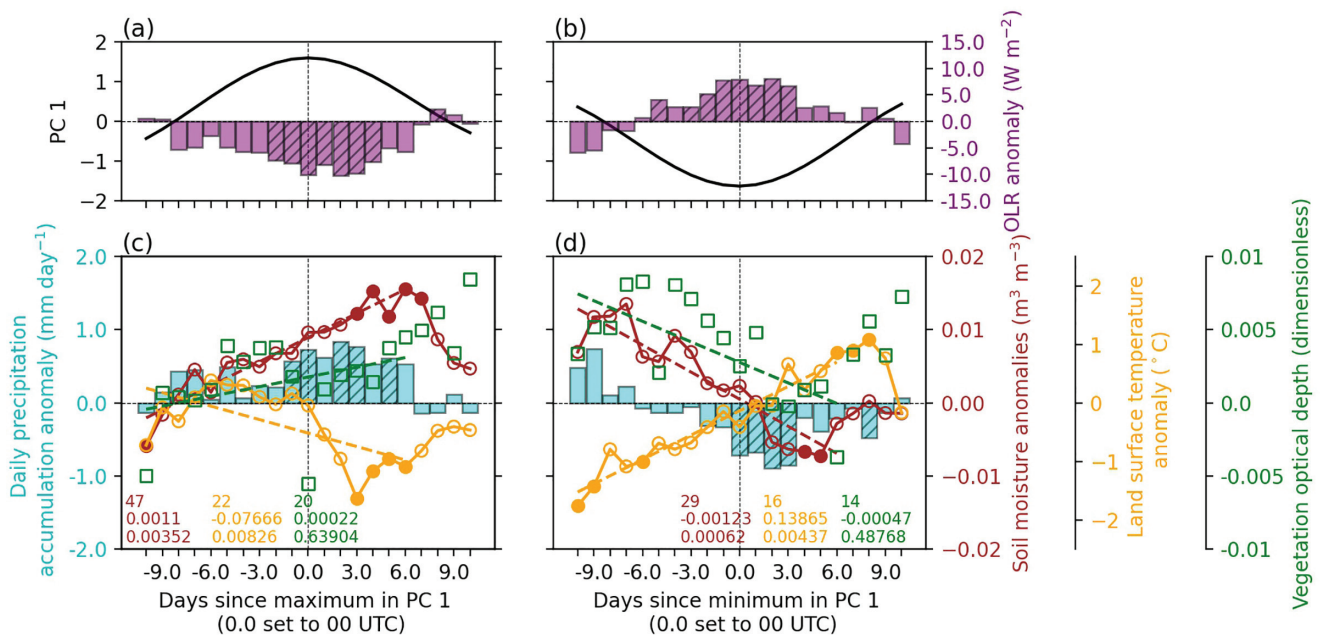


FIGURE 3 (a, b) Composite-mean PC1 values (black line, dimensionless) and Sahelian-mean (12–18°N, -15 to 20°E) OLR anomalies (purple bars, $W \cdot m^{-2}$) in (a) wet and (b) dry intraseasonal event composites. (c, d) Composite-mean, Sahelian-mean anomalies in daily-accumulated precipitation (cyan bars, $mm \cdot day^{-1}$), surface soil moisture (dotted brown line, $m^3 \cdot m^{-3}$), LST (dotted yellow line, $^{\circ}C$), and VOD (green squares, dimensionless) in (c) wet and (d) dry intraseasonal event composites. Significant anomalies at the 95% confidence level are denoted by hatching or filled markers. Dashed lines denote evolution in soil moisture (brown, $m^3 \cdot m^{-3} \cdot day^{-1}$), LST (yellow, $^{\circ}C \cdot day^{-1}$), and VOD (green, day^{-1}) between days -10 and +6 of each composite. The number of events in each composite, linear regression gradient, and two-sided *p*-value of the regression line is labelled in each panel where the text colour is consistent with each variable. Sahelian-mean observations during a single day of an intraseasonal event are only included if at least 25% of the Sahel region contains observations. Dashed black horizontal and vertical lines denote the zero value

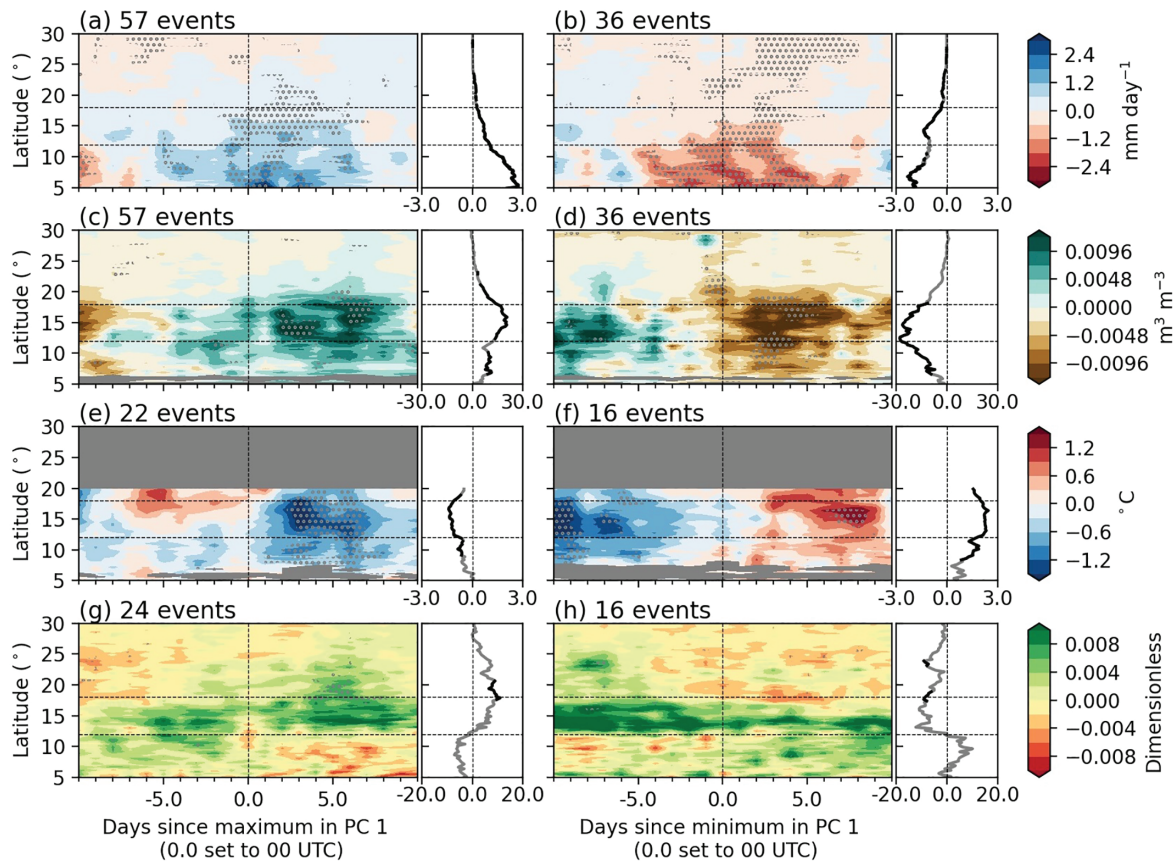


FIGURE 4 Composite-mean Hovmöller diagrams (averaged between -15 and 20°E) in anomalous (a, b) precipitation ($\text{mm}\cdot\text{day}^{-1}$), (c, d) soil moisture ($\text{m}^3\cdot\text{m}^{-3}$), (e, f) LST ($^{\circ}\text{C}$), and (g, h) VOD (dimensionless) for (left) wet and (right) dry intraseasonal event composites. Grey circles denote significance at a 95% confidence level. The line plot shown to the right of each panel denotes the evolution of each variable between days -10 and $+6$ where a black line denotes significance at a 95% confidence level. In the case for soil moisture and VOD, the evolution has been multiplied by 1,000. Dashed black horizontal lines denote the latitudinal region (12 to 18°N) averaged for the Sahel-mean in Figure 3, whilst dashed black vertical lines denote the zero value

and dry event evolution. Significant changes in soil moisture and LST are observed in both composites across the 17 days. For example, the surface warms by approximately 2°C during a dry event, and cools by approximately 1.5°C during a wet event. Whilst statistically insignificant at a 95% confidence level, we also observe consistent changes in VOD with a greening of the Sahel during wet events and a vegetation reduction during dry events. A qualitatively similar surface response is observed when only analysing events that occur in the common time span of all satellite products (2004 to 2018; not shown).

Hovmöller diagrams of anomalous precipitation, soil moisture, and LST illustrate a meridional variation in the surface response to intraseasonal events. The dry and wet evolution at each latitude highlights that, whilst precipitation changes are smaller across the Sahel than the Guinea coast and Sudan Savannah (Figure 4a,b), perturbations in soil moisture and LST are strongest across the Sahel (Figure 4c–f). Predominately dry soils, the intermittent frequency of storms (≈ 3 to 4 days), and a high

evaporative demand across the Sahel, drive stronger temporal variability in surface soil moisture than in regions further south (Figure 4c,d) where the surface is close to saturation and rarely dries out during periods of rainfall deficiency. Due to low soil moisture content across the Sahel, variations in soil moisture control the partitioning of surface turbulent fluxes and therefore land surface temperatures (Figure 4e,f). We also note qualitatively similar precipitation anomalies during intraseasonal events in other products including the Integrated Multi-satellite Retrievals for GPM (IMERG; Huffman *et al.*, 2019) and the Tropical Rainfall Measuring Mission (TRMM) version 3B42 (Huffman *et al.*, 2016, not shown). Alongside perturbations in soil moisture and LST, VOD observations highlight a vegetation response (Figure 4g,h). For example during dry events, vegetation decreases across the Sahel with significant changes across parts of the northern Sahel and Sahara (Figure 4h). The vegetation response is likely to amplify and prolong changes in surface turbulent fluxes associated with surface soil moisture perturbations,

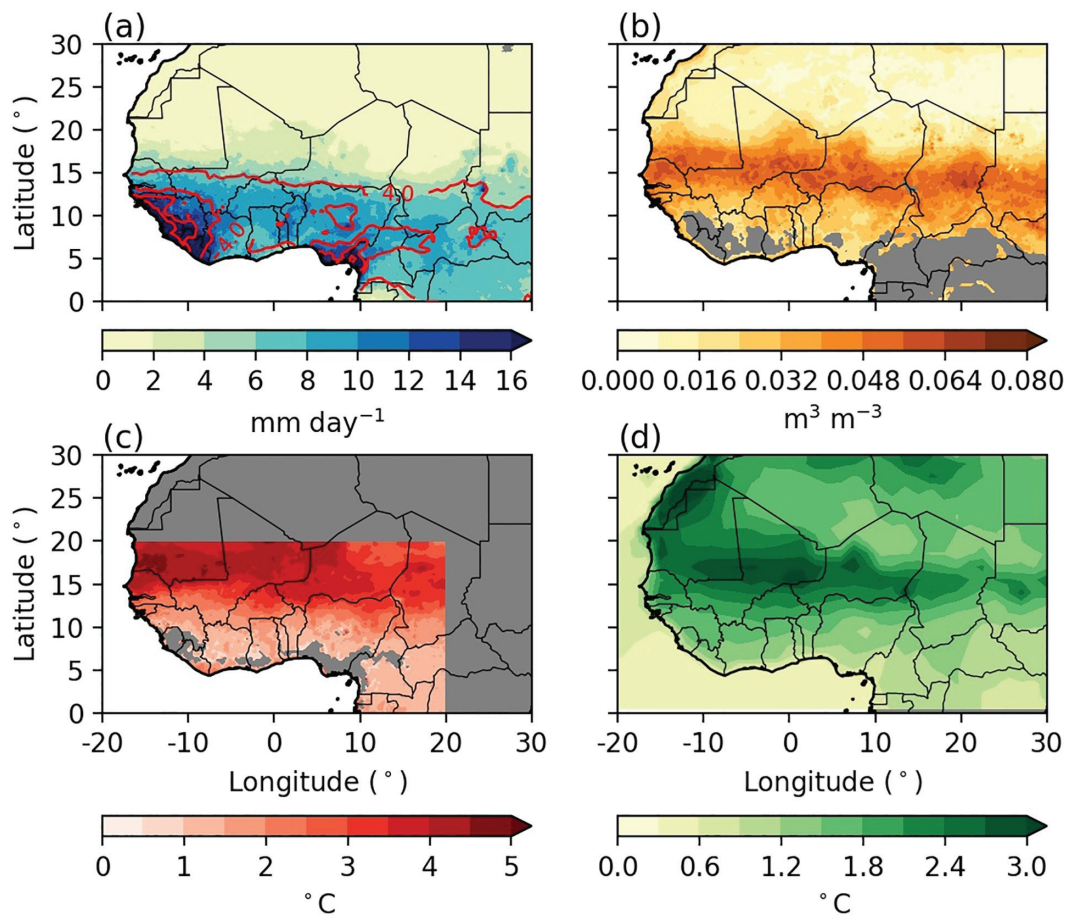


FIGURE 5 Composite-mean standard deviation in (a) precipitation ($\text{mm}\cdot\text{day}^{-1}$), anomalous (b) soil moisture ($\text{m}^3\cdot\text{m}^{-3}$), (c) LST ($^{\circ}\text{C}$) and (d) 1800 UTC near-surface air temperature ($^{\circ}\text{C}$) during all 20 days in the dry and wet intraseasonal event composites. Red contours on (a) denote the climatology of CHIRPS precipitation during the monsoon season at intervals of $4\text{ mm}\cdot\text{day}^{-1}$

as vegetation has access to moisture within the root zone.

To further isolate the locations across West Africa where the surface response to intraseasonal variability is particularly pronounced, we compute the standard deviation of observations within ± 10 days of a maximum or minimum in PC1 at each grid point. Figure 5 shows the composite-mean standard deviation when averaging across all dry and wet events. We also show the rainfall climatology when the West African monsoon is fully active (Figure 5a). Again, it is evident that soil moisture and LST variations are most substantial across the Sahel, even though rainfall variability is larger across southern West Africa (Figure 5a–c). The coherent zonal band in soil moisture and LST variations highlights a region where surface turbulent fluxes are sensitive to surface soil moisture, and intraseasonal rainfall variability is large enough to impact the surface energy balance. Across the Sahel, evapotranspiration is limited by surface moisture, leading to a LST and surface energy balance response to precipitation

variations (Lohou *et al.*, 2014). Meanwhile across the Guinea coast and Sudan Savannah, climatologically wet conditions makes evapotranspiration more controlled by radiation rather than surface soil moisture. The strong meridional gradient over West Africa in the control of soil moisture on surface fluxes is consistent with previous studies that have shown that the Sahel is a hotspot for land–atmosphere coupling (i.e., Guo *et al.*, 2006; Dirmeyer, 2011; Miralles *et al.*, 2012; Gallego-Elvira *et al.*, 2016).

Performing the same analysis on ERA5 1800 UTC near-surface air temperatures highlights that the low-level atmosphere is also sensitive to intraseasonal variability across the Sahel (Figure 5d). This suggests that the moisture-induced LST response across the Sahel feeds back onto the local atmosphere. Note that in parts of the northern Sahara, substantial variability in air temperature is not linked to surface hydrology, and is more likely driven by heat advection from coherent circulation anomalies. In the following section we investigate whether intraseasonal surface perturbations feed back onto the dynamics of the

West African monsoon circulation (Section 4.1) and affect characteristics of deep convection (Section 4.2).

4 | INTRASEASONAL SOIL MOISTURE– ATMOSPHERE FEEDBACKS

4.1 | Regional atmospheric response to intraseasonal surface perturbations

In the previous section we identified a coherent, regional-scale surface response to intraseasonal rainfall variability across West Africa. Here, we investigate whether the surface response feeds back onto the monsoon circulation. Hovmöller diagrams of composite-mean low-level atmospheric temperatures averaged across West Africa (-15 to 20°E) reveal anomalous atmospheric conditions during intraseasonal events (Figure 6a,d). Two lines of evidence support the argument that these anomalous temperatures are caused by surface changes and their influence on the partitioning of surface turbulent fluxes. Firstly, using the dry event composite as an example, significant warming is observed across the Sahel (Figure 6a) which is consistent with surface drying and heating (Figure 4d,f). Secondly, anomalous low-level temperatures exhibit a striking diurnal cycle with the dry

event evolution peaking at just under 2°C at 1800 UTC (Figure 6b). To illustrate the diurnal cycle of temperature anomalies further, we also show the three-hourly composite-mean anomalous warming rate during days 0 to 5 (Figure 6c,f). In the dry event composite, anomalous warming at 925 hPa occurs between 0900 and 1800 UTC (Figure 6c). During these hours, temperatures at 925 hPa are typically within the well-mixed daytime boundary layer and influenced by enhanced surface sensible heat fluxes. Meanwhile, during the night anomalous temperatures in the residual layer dissipate due to surface fluxes being close to zero. The diurnal cycle of warming rates clearly indicates that daytime anomalous surface heat fluxes are the cause for low-level temperature variability as climatological warming rates are positive between 0900 and 1500 UTC, and negative at other times of the day (not shown). During a dry event between 1500 and 1800 UTC, the anomalous warming rate is positive and similar to rates observed at midday, indicating reduced cooling, relative to the climatology, during the late afternoon (Figure 6c). This sustained anomalous heating highlights a decoupling from daytime peak radiation and that anomalous soil moisture drives enhanced surface sensible heat fluxes and the accumulation of heat within the boundary layer. We also observe anomalous temperatures propagating northwards with the nocturnal monsoon flow (Figure 6a,d; Parker *et al.*, 2005). Zonal-mean temperature trends

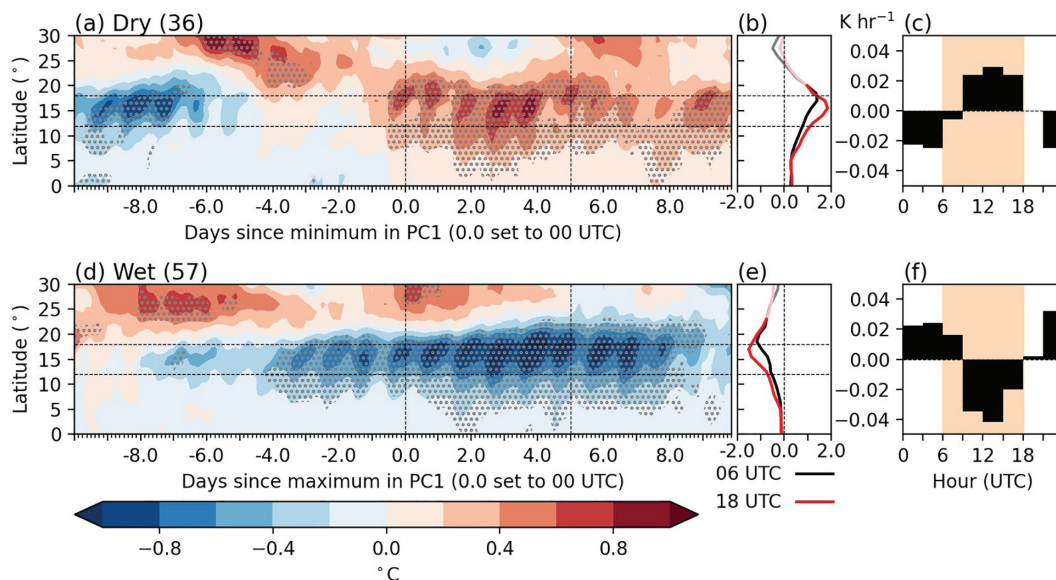


FIGURE 6 (a,d) Hovmöller diagrams of composite-mean, zonal-mean (-15 to 20°E) anomalous 925 hPa temperatures ($^{\circ}\text{C}$), (b, e) temperature evolution at 0600 (black) and 1800 (red) UTC, and (c, f) Sahelian-mean (12 – 18°N , -15 to 20°E) anomalous 925 hPa temperature warming rates ($\text{K}\cdot\text{hr}^{-1}$) between days 0.0 and 5.0 during (a–c) dry and (d–f) wet events. On (a, d), grey stippling denotes 95% significance. Dashed black horizontal lines on (a, b) and (d, e) denote the latitudinal region averaged for Sahelian-mean whilst on (a, d) dashed black vertical lines denote the time period used for calculating average warming rates. The number of events in each composite is shown in the titles of (a) and (c). Opaque lines on (b, e) denote significance at a 95% confidence level. On (c, f) daytime hours (0600 to 1800 UTC) are shaded light orange

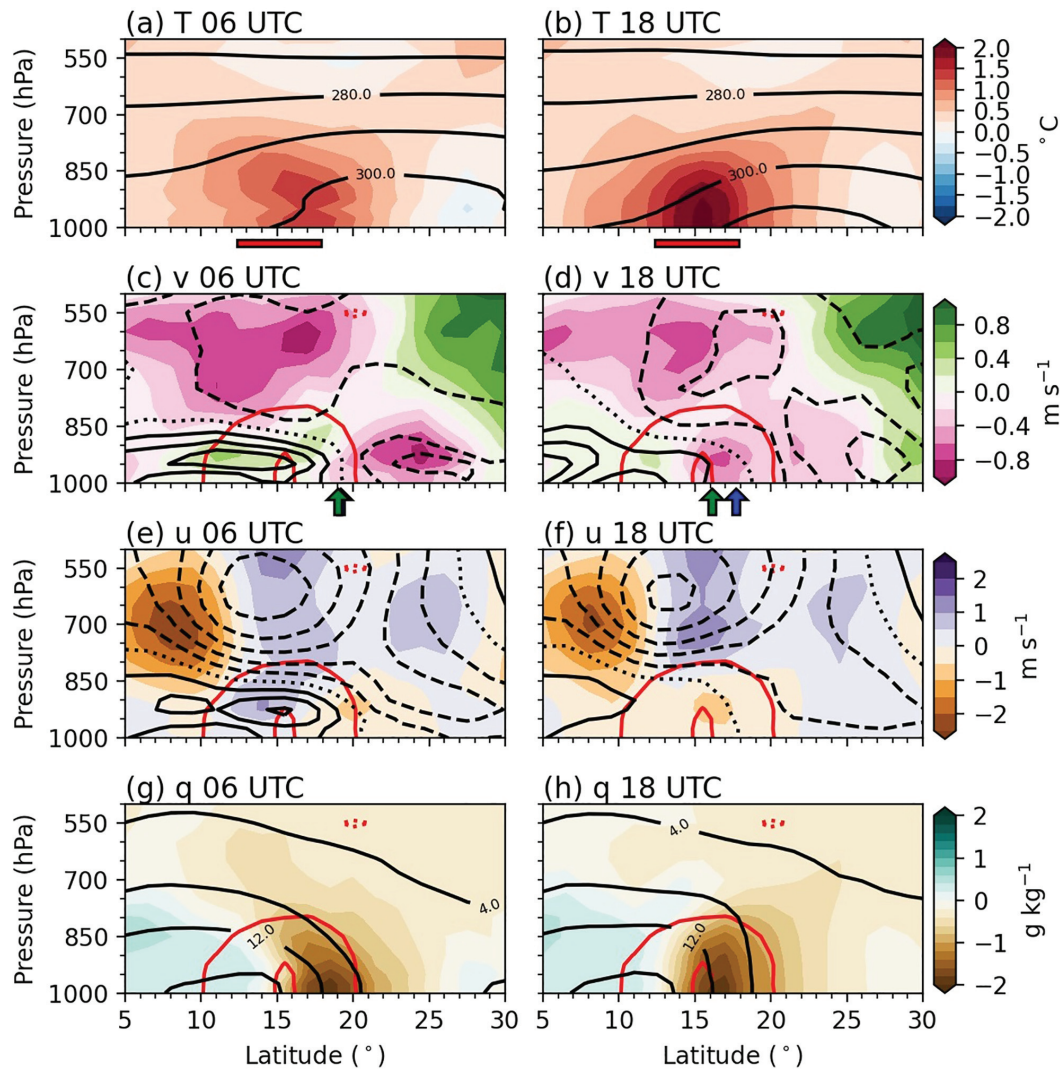


FIGURE 7 Composite-mean, zonal-mean (-15 to 20°E) vertical profile of climatology (contours) and dry event (shading) evolution in (a, b) temperature ($^{\circ}\text{C}$), (c, d) meridional wind ($\text{m}\cdot\text{s}^{-1}$), (e, f) zonal wind ($\text{m}\cdot\text{s}^{-1}$), and (g, h) specific humidity ($\text{g}\cdot\text{kg}^{-1}$) at (a, c, e, g) 0600 and (b, d, f, h) 1800 UTC. Intervals of 10°C , $1\text{ m}\cdot\text{s}^{-1}$, $2\text{ m}\cdot\text{s}^{-1}$, and $4\text{ g}\cdot\text{kg}^{-1}$ are used for the climatology of temperature, meridional wind, zonal wind, and specific humidity respectively. Solid (dashed) lines denote positive (negative) values. The zero value is denoted by a dotted contour. In (c–h) red lines denote the dry event evolution of temperature ($^{\circ}\text{C}$) at 1800 UTC at intervals of 1.0°C . The red rectangles below (a, b) highlight latitudes with an LST dry event evolution greater than 2°C . Arrows below (c, d) denote the approximate location of the ITD in climatology (blue) and when adding the evolution of meridional wind during a dry event (green). Below (c) the green arrow almost coincides with the blue arrow

coincide with decreased and increased mean sea level pressure of approximately 1 hPa across the Sahel during dry and wet events respectively (not shown). This implies a dynamical atmospheric response to surface changes and that intraseasonal soil moisture variations may feed back onto the dynamics of the monsoon circulation.

To understand the atmospheric response to surface-induced heating anomalies, Figure 7 shows the zonal-mean vertical profile of the dry event evolution for temperature, horizontal wind, and specific humidity at 0600 and 1800 UTC (shading) along with the climatology (lined). Increased surface temperatures, driven

by reduced soil moisture, lead to atmospheric warming that is confined to the planetary boundary layer and maximises at 1800 UTC (Figure 7a,b). Changes in low- and mid-tropospheric winds show that anomalous surface-induced boundary-layer heating leads to a southward shift of the shallow meridional circulation (Figure 7c–f). Monsoon southwesterlies are enhanced to the south of surface-driven warming, associated with an increased meridional temperature gradient, whilst low-level northeasterlies are promoted to the north. This meridional perturbation of the monsoon circulation shifts the ITD southwards by approximately 1.5° latitude

(Figure 7d). In this study the location of the ITD has been approximated using the interpolated location where the 925 hPa meridional wind speed equals zero. The low-level wind response maximises at 0600 UTC and is suppressed during the daytime due to daytime surface warming promoting boundary-layer turbulence which prohibits a wind response to the surface-induced pressure gradient. This is consistent with Parker *et al.* (2005) who showed that West African monsoon winds maximise overnight when the convective boundary layer is diminished and boundary-layer turbulence is weak. The diurnally varying atmospheric response is similar to those found in modelling (Rácz and Smith, 1999; Smith and Spengler, 2011) and observational (Hoinka and Castro, 2003; Parker *et al.*, 2005; Howard and Washington, 2018; Talib *et al.*, 2021) studies of the dynamical atmospheric response to surface warming in the Sahel and other regions of the world. The southward monsoon shift also leads to substantial humidity perturbations with specific humidity decreasing by up to $1.6 \text{ g}\cdot\text{kg}^{-1}$ to the north of maximum warming (Figure 7h). The co-location of the peak humidity reduction with maximum northerly wind anomalies at approximately 17°N (Figure 7d,h) implies that the humidity evolution to the north of the ITD is primarily controlled by circulation changes rather than changes in evapotranspiration.

In addition to a low-level wind response to surface warming, the AEJ shifts southwards during a dry event (Figure 7e,f). Through thermal wind balance, vertical wind shear is directly proportional to the meridional temperature gradient. In the climatology, a positive meridional temperature gradient is observed between 5 and 20°N which is associated with an easterly wind shear and an AEJ located at 13°N . Low-level warming shifts the maximum in the meridional temperature gradient southwards (Figure 7b), thereby promoting a southward shift of the AEJ (Figure 7f). The height of the AEJ maximum occurs where the meridional temperature gradient changes from positive to negative (Cook, 1999; Thorncroft and Blackburn, 1999). In our dry event composite, the evolution of the meridional temperature gradient changes sign at approximately 700 hPa at 15°N (Figure 7b). As 700 hPa is approximately 100 hPa below the climatological AEJ location, the AEJ is promoted closer to the surface (Figure 7e,f). The southward shift of the AEJ during dry events is consistent with work by Newell and Kidson (1984) and Shekhar and Boos (2017), who both show that the shallow meridional circulation across West Africa shifts northward during wet years across the Sahel. Shekhar and Boos (2017) also observe cooling below 700 hPa over the Sahel during wet years which is hypothesised to be caused by surface cooling and reduced surface sensible heat fluxes. Note that differences

in characteristics of the AEJ at 0600 and 1800 UTC are smaller than differences in low-level monsoon westerlies (Figure 7c–f), as mid-tropospheric winds are not restricted by frictional forces induced by surface turbulent fluxes.

To understand spatial variations in the atmospheric response to anomalous surface conditions, figure 8 shows maps of the atmospheric evolution during intraseasonal events. Focusing on dry events, surface-induced zonally oriented low-level warming across the Sahel leads to intensified low-level northeasterlies and monsoon southwesterlies across the Sahel and Sudan Savannah (Figure 8b). Through showing the evolution of the difference in wind speed at 925 and 600 hPa, figure 8d highlights that the combination of stronger monsoon southwesterlies with an expanded, intensified, and southward-shifted AEJ, increases low-tropospheric wind shear across the Guinea coast. Low-level moistening is also observed across the Guinea coast and Sudan Savannah which may be linked to an increased moisture flux from the Gulf of Guinea or a change in the frequency of deep convection (Figure 8f). Figure 9 is a schematic highlighting the key atmospheric changes during a dry event. Surface-induced low-level atmospheric warming across the Sahel intensifies monsoon southwesterlies and dry northeasterlies, shifts the ITD southwards, and intensifies the AEJ. Whilst in this study we have mostly discussed soil moisture–atmosphere feedbacks during dry events, as previous work has shown that intraseasonal dry phases are larger in magnitude than wet phases (Pohl *et al.*, 2009), figure 8 highlights that soil moisture–atmosphere feedbacks during wet events can also lead to significant atmospheric changes.

4.2 | Response of convective storms to intraseasonal surface perturbations

Previous work has shown that intense convection is more likely in regions where the AEJ is strong (Mohr and Thorncroft, 2006), and that the genesis and intensification of mesoscale convective systems (MCSs) is favoured in southern regions of temporary southward excursions of the ITD where low-level convergence is enhanced (Vizy and Cook, 2018; Klein and Taylor, 2020). Furthermore, the intensification of MCSs has been found to be favoured over dry soils due to an enhanced meridional temperature gradient which in turn accelerates the AEJ and increases zonal wind shear (Klein and Taylor, 2020). Therefore, we hypothesise that increased low-tropospheric shear (Figure 8d), driven by surface-induced low-level atmospheric warming across the Sahel (Figure 8b), leads to stronger deep convection across southern West Africa. In this subsection, we investigate how properties of deep convection change during intraseasonal events.

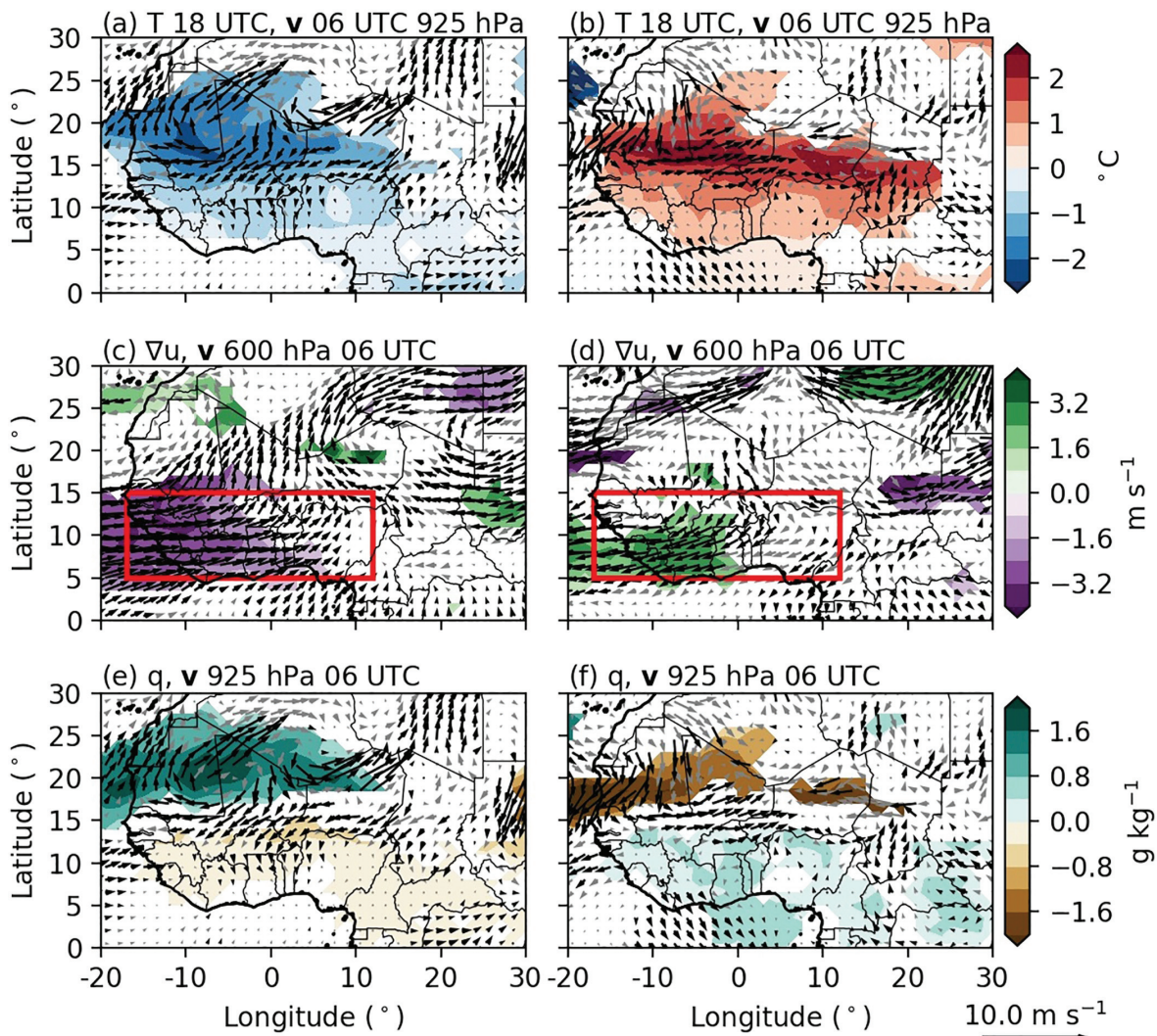


FIGURE 8 Evolution in (a, b) 925 hPa 1800 UTC temperature (shading, $^{\circ}\text{C}$), (c, d) 0600 UTC low-tropospheric zonal wind shear (shading, $\text{m}\cdot\text{s}^{-1}$), and (e, f) 925 hPa 0600 UTC specific humidity (shading, $\text{g}\cdot\text{kg}^{-1}$) during (a, c, e) wet and (b, d, f) dry events. Values are only shown if significant at the 90% confidence level. The evolution of horizontal wind at 0600 UTC (a, b, e, f) 925 hPa and (c, d) 600 hPa is also shown (arrows, $\text{m}\cdot\text{s}^{-1}$) with significant values at the 90% confidence level, in either a zonal or meridional direction, denoted by black arrows. Grey arrows are used to denote insignificant wind changes. The red rectangle in (c, d) denotes the region (5 to 15°N , -17 to 12°E) used for analysing deep convection in Section 4.2

To identify changes in characteristics of deep convection, we generate a composite of convective storms at 1800 UTC on a 1° latitude by 1° longitude grid across southern West Africa (5 – 15°N , -17 to 12°E ; region highlighted in Figure 8c,d) using thermal infrared brightness temperatures (Section 2.1). For every day across each grid box we compute the percentage area covered by cloud-top temperatures $< -40^{\circ}\text{C}$ and the mean minimum temperature associated with each convective storm. As storm intensity and frequency across southern West Africa vary seasonally (Klein *et al.*, 2021), a 30-day rolling mean of the average annual cycle in each grid box is subtracted. Figure 10 shows the zonal-mean evolution in minimum cloud-top temperature and cloud area. Note

that the zonal-mean calculation is weighted by the number of convective cores in each grid box. Increased and decreased cloud-top temperatures correspond to weakened and intensified deep convection respectively. South of 12°N , deep convection intensifies during dry events with minimum cloud-top temperatures decreasing by approximately 2.0°C (Figure 10b). As expected with a dry event, the cloud area decreases by approximately 20% (Figure 10b). Therefore, whilst deep convection occurs less frequently as a dry event progresses, when it does occur, convection is more intense. On the other hand, the weakening of storms across southern West Africa during wet events is relatively weak and mostly insignificant (Figure 10a).

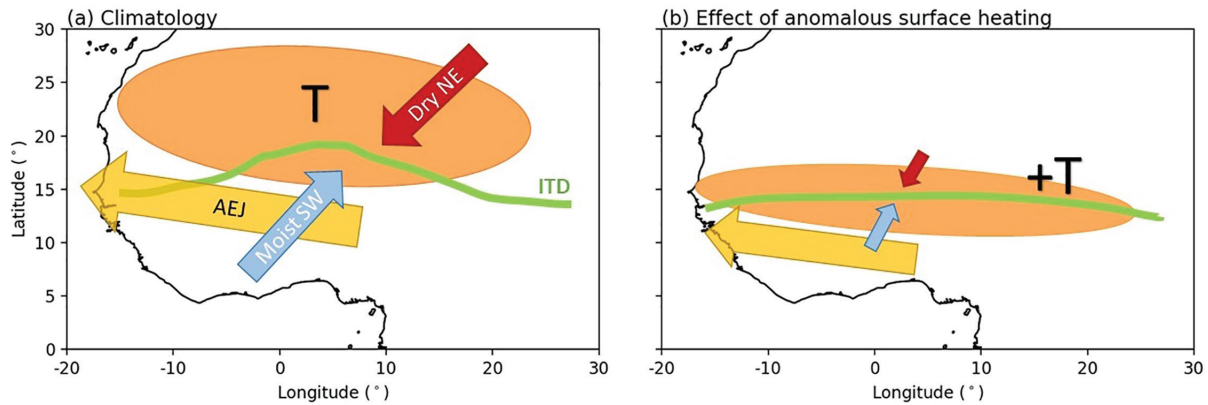


FIGURE 9 Schematic illustrating (a) climatological conditions across West Africa when the monsoon is active and (b) the impact of anomalous surface heating during a dry event. Low-level warming across the Sahara is denoted by an orange oval whilst moist southwesterlies and dry northeasterlies are denoted by blue and red arrows respectively. The AEJ is shown by a yellow arrow whilst the ITD location and shape is denoted by a green line. In (b) ovals and arrows are used to denote temperature and wind perturbations, whilst the green line denotes the new ITD location and shape

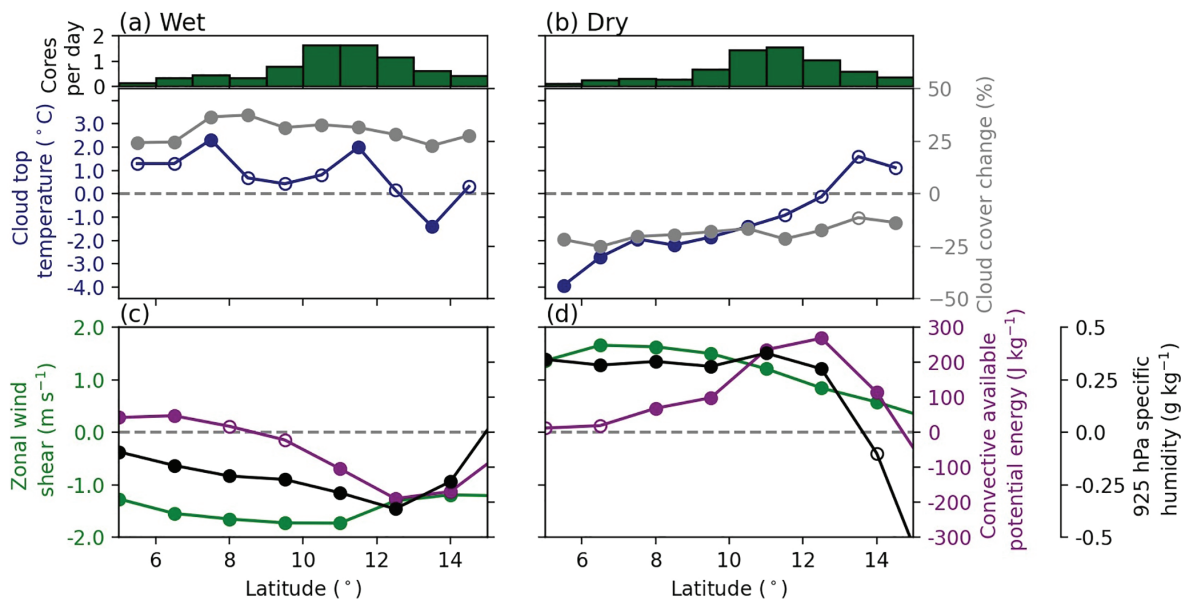


FIGURE 10 (a, b) Zonal-mean (-17 to 12°E) evolution in anomalous 1800 UTC cloud-top temperatures (blue, $^{\circ}\text{C}$) and percentage change in cloud cover (grey, %) when using a -40°C temperature threshold in (a) wet and (b) dry events. The zonal-mean calculation for anomalous cloud-top temperature is weighted by the number of convective storms analysed at each longitude with green bars above each panel denoting the average number of convective storms analysed at each latitude per day. (c, d) Zonal-mean (-17 to 12°E) evolution in 1200 UTC low-level (925–600 hPa) zonal wind shear (green, m s^{-1}), surface CAPE (purple, J kg^{-1}), and 925 hPa specific humidity (black, g kg^{-1}) in (c) wet and (d) dry events. Filled markers denote values which are significant at the 90% confidence level

To understand the drivers of the intensification of convection during dry events (Figure 10b), we analyse the zonal-mean evolution of anomalous 1200 UTC surface convective available potential energy (CAPE), low-level humidity, and low-tropospheric shear (Figure 10d). South of 12°N , the intensification of convection is strongly associated with increased shear and low-level specific humidity. In contrast, the meridional signature

of CAPE does not resemble that of cloud-top temperatures, implying that CAPE is not driving the observed evolution in convection intensity. To summarise, a southward shift of the shallow monsoon circulation, induced by surface drying during an intraseasonal dry event, increases zonal wind shear and moisture across southern West Africa, which promotes an intensification of convection.

5 | DISCUSSION

In this study we show that soil moisture–atmosphere feedbacks play a crucial role in regional-scale, intraseasonal fluctuations of the West African monsoon circulation. The large-scale surface response to intraseasonal variability across West Africa is similar to the surface response observed in India and other tropical regions (Saha *et al.*, 2012; Sathyanadh *et al.*, 2016; Peng *et al.*, 2017). Surprisingly, even though daily rainfall during the West African monsoon is highly variable, both spatially and temporally, a coherent regional-scale surface response to intraseasonal variability is observed. Across West Africa, differences in soil moisture content lead to differences in how surface turbulent fluxes respond to anomalous precipitation, with the response being strongest across the Sahel where surface water is limited (Timouk *et al.*, 2009; Lohou *et al.*, 2014; Gallego-Elvira *et al.*, 2016). Meridional differences in the surface response to intraseasonal precipitation variability plays a crucial role in the observed impact on the dynamics of the West African monsoon. We find that an intraseasonal dry event leads to regional-scale surface drying across the Sahel with an associated southward shift of the West African monsoon circulation by approximately 1.5° latitude. This study provides new insight into how intraseasonal, regional-scale rainfall variability can impact the dynamics of a monsoon circulation and highlights the importance of soil moisture–atmosphere feedbacks therein.

Our analysis indicates that soil moisture–atmosphere interactions induce an internal feedback that affects the evolution of intraseasonal events across West Africa. During an intraseasonal dry event, reduced soil moisture increases the meridional temperature gradient in the southern Sahel, which leads to a strengthened, southward-shifted AEJ and enhances low-level shear. A strengthened AEJ favours the intensification of convection (Klein and Taylor, 2020), whilst increased instability, through low-level warming and increased shear, supports the triggering, growth, and propagation of AEWs (Hall *et al.*, 2006; Hsieh and Cook, 2008; Thorncroft *et al.*, 2008; Leroux and Hall, 2009; Russell *et al.*, 2017). Both of these mechanisms counteract the external forcing which initiates the regional-scale dry spell. We therefore speculate that soil drying acts as a negative feedback which weakens the original intraseasonal forcing across the Guinea coast and Sudanian Savannah. Along with soil moisture–atmosphere feedbacks affecting the within-event evolution of the current intraseasonal state, it may also be the case that these feedbacks impact the following intraseasonal phase. For example, Saha *et al.* (2012) showed that a dry intraseasonal phase of the Indian monsoon leads to surface drying and increased atmospheric

instability, which promotes convection and an intensification of the following wet intraseasonal event. As a result, intense dry intraseasonal events are followed by strong wet intraseasonal events. Such feedbacks may also affect the intensity of intraseasonal variability in West Africa, including variability across shorter time-scales such as the ‘Sahel’ mode (Taylor, 2008; Janicot *et al.*, 2011), which future studies could address.

Regarding the timing of intraseasonal events, our study considers intraseasonal variability only during the active phase of the West African monsoon as we explicitly ignore cases before and around the monsoon onset. However, given that monsoon onset regularly occurs during a dry intraseasonal event (Sultan and Janicot, 2003), it may be the case that soil moisture feedbacks support the onset of the West African monsoon alongside atmospheric drivers (Sultan and Janicot, 2003; Gu and Adler, 2004; Hagos and Cook, 2007; Flaounas *et al.*, 2012). The West African monsoon onset, which typically occurs in mid-June to early-July, is defined by an abrupt meridional precipitation shift from 5 to 10°N and is preceded by a strong heat low circulation at 15°N that drives low-level monsoon westerlies and inland moisture advection (Sultan and Janicot, 2000; 2003; Hagos and Cook, 2007; Lavaysse *et al.*, 2009). In this study we have shown that soil moisture–atmosphere feedbacks contribute to the regional cessation of dry intraseasonal events. We therefore hypothesise that related mechanisms may promote the monsoon onset when occurring ahead of the monsoon season. This hypothesis is supported by Berg *et al.* (2017), who showed that prescribing a fixed seasonal cycle of soil moisture in the latest state-of-the-art general circulation models (GCMs) promotes near-surface cooling, due to enhanced surface evapotranspiration, and delays the monsoon onset across the Guinea coast. In future work, we hope to quantitatively diagnose the influence of soil moisture–atmosphere feedbacks on the West African monsoon onset.

The effect of intraseasonal soil moisture–atmosphere feedbacks on the dynamics of the West African monsoon encourages a global assessment of intraseasonal surface–atmosphere feedbacks as strong intraseasonal precipitation variability is observed in other tropical regions (Pohl and Camberlin, 2006; Waliser, 2006; Chikoore and Jury, 2010; Wang *et al.*, 2012). Whilst Peng *et al.* (2017) shows a soil moisture response to MJO-induced variability in other parts of the Tropics, it still remains to be investigated whether the soil moisture response feeds back onto the atmosphere. Studies which have used observations to analyse tropical intraseasonal land–atmosphere feedbacks are few in number (Saha *et al.*, 2012; Chug and Dominguez, 2019). Whilst in this study we mainly focus on soil moisture–atmosphere feedbacks, we also identify a

vegetation response to intraseasonal variability across the northern Sahel and Sahara. It may be the case that this vegetation response acts as a source of predictability for future weather conditions. For example, previous research has suggested that increased vegetation across the Sahel during September to November promotes rainfall through enhanced evapotranspiration (Yu *et al.*, 2017).

Considering modelling implications of our findings, the latest coupled GCMs show substantial inter-model variability in the soil moisture and surface turbulent flux response to precipitation across West Africa (Koster *et al.*, 2006; Lohou *et al.*, 2014; Gallego-Elvira *et al.*, 2019). The inter-model variability in the surface turbulent flux response to precipitation is greater over bare soil than vegetated surfaces (Lohou *et al.*, 2014). When comparing with observations that show Sahelian surface warming and substantial meridional differences in the surface response to a prolonged dry spell (Gallego-Elvira *et al.*, 2016), it is evident that most GCMs either have insufficient surface warming or lack a meridional variation in the surface response (Gallego-Elvira *et al.*, 2019). As a result, it is likely that most models poorly represent intraseasonal land–atmosphere feedbacks as without surface warming or a meridional variation in the surface response, a shift of the monsoon circulation will not be represented. As well as models poorly simulating the surface response to precipitation variability, there is also substantial inter-model spread in the variance of near-surface air temperature and precipitation explained by soil moisture, with Notaro *et al.* (2020) suggesting that most models underestimate the influence of soil moisture. Consequently, caution should be taken when investigating soil moisture–atmosphere feedbacks in climate models, as the sign and magnitude of the simulated soil moisture–precipitation feedback is sensitive to the representation of convection, choice of circulation model, and atmospheric resolution (Hohenegger *et al.*, 2009; Taylor *et al.*, 2013). Evaluations of the first convection-permitting climate simulation over Africa also reveal an insufficient sensitivity of modelled convective storms to ambient wind shear, suggesting that storm–shear interactions may be difficult to capture even for some higher-resolution models (Senior *et al.*, 2021). As a result, it may be the case that numerical weather prediction models poorly simulate the response of convective storms to shear changes associated with intraseasonal soil moisture–atmosphere feedbacks.

Finally, through better understanding intraseasonal soil moisture–atmosphere feedbacks during the West African monsoon, we can support efforts to improve subseasonal forecasts of the large-scale circulation and help reduce the impacts of hydrometeorological extreme events. Intraseasonal surface changes can impact crop yields, however regularly adjusting agricultural practices,

such as date of sowing, and improving the communication of subseasonal forecasts can minimise losses (Sultan *et al.*, 2005; Lawal *et al.*, 2021). The atmospheric response to intraseasonal soil moisture–atmosphere feedbacks has been shown to influence characteristics of deep convection. Hence, acknowledging the current intraseasonal state can improve the actions taken to minimise the impacts of anomalous surface conditions and intense convection. The improved knowledge of intraseasonal land–atmosphere feedbacks from this study encourages weather and climate model evaluation which will ultimately improve forecasting capabilities and the actions taken by forecast users.

6 | CONCLUSIONS

Using multiple satellite products and an atmospheric reanalysis, we have shown a coherent, regional-scale surface response in the water-limited Sahel to intraseasonal precipitation variability across West Africa. In spite of relatively weak intraseasonal precipitation variability in West Africa than in other tropical regions, a clear soil moisture–atmosphere feedback is observed. The feedback during an intraseasonal dry event intensifies and shifts the band of intermittent convection southwards. Considering soil moisture–atmosphere feedbacks as an internal feedback in response to an external atmospheric forcing, observations show that intraseasonal soil moisture fluctuations drive a negative feedback to the original precipitation anomaly. The impact of reduced soil moisture and evapotranspiration across southern West Africa on convection during a dry event is overcome by the dynamical atmospheric response to a southward-shifted meridional temperature gradient. Convection-permitting numerical modelling experiments, which simulate more realistic rainfall and a negative feedback between soil moisture and rainfall, are required to fully understand the influence of soil moisture–atmosphere feedbacks on the longevity and intensity of intraseasonal variability across West Africa. Future work should also investigate the atmospheric response to intraseasonal land–atmosphere feedbacks in other parts of the world, and evaluate intraseasonal surface–atmosphere feedbacks in weather and climate models.

ACKNOWLEDGEMENTS

This work and several contributors (JT, CT, VS) were supported by UK Research and Innovation (UKRI) as part of the Global Challenges Research Fund, African Science for Weather Information and Forecasting Techniques (SWIFT) programme, grant number NE/P021077/1. CK and SA were funded from the United Kingdom's Natural

Environment Research Council (NERC)/Department for International Development (DFID) Future Climate For Africa program under the African Monsoon Multidisciplinary Analysis-2050 (AMMA-2050) project (grant number NE/M020428/2), and the NERC/DFID Nowcasting Flood Impacts of Convective Storms in the Sahel (NFLICS) project (grant number NE/S006087/1) respectively. BH was supported by UKRI under the National Centre for Earth Observation (NCEO) Long Term Science Single Centre (LTSS) project, grant number NE/R016518/1. We would also like to thank two anonymous reviewers for their comments which substantially improved this study.

All datasets used in this study are freely available. ESA CCI soil moisture satellite observations and VOD data were accessed at www.esa-soilmoisture-cci.org and <https://doi.org/10.5281/zenodo.2575599> respectively. Meteosat First and Second Generation satellite data were accessed through www.eumetsat.int. Interpolated OLR data were provided by the NOAA, Boulder, Colorado, USA, from their web site at https://psl.noaa.gov/data/gridded/data.interp_OLR.html, whilst CHIRPS precipitation can be downloaded at <https://www.chc.ucsb.edu/data/chirps>. ERA5 data were accessed on <https://cds.climate.copernicus.eu/cdsapp/#/> home (all accessed 29 March 2022).

AUTHOR CONTRIBUTIONS

Joshua Talib: conceptualization; data curation; formal analysis; investigation; methodology; visualization; writing – original draft; writing – review and editing. **Christopher M. Taylor:** conceptualization; data curation; funding acquisition; methodology; supervision; visualization; writing – original draft; writing – review and editing. **Cornelia Klein:** conceptualization; data curation; methodology; writing – review and editing. **Bethan L. Harris:** data curation; methodology; visualization; writing – review and editing. **Seonaid R. Anderson:** Valiyaveetil S. Semeena: data curation.

ORCID

Joshua Talib  <https://orcid.org/0000-0002-4183-1973>

Christopher M. Taylor  <https://orcid.org/0000-0002-0120-3198>

Cornelia Klein  <https://orcid.org/0000-0001-6686-0458>

Bethan L. Harris  <https://orcid.org/0000-0002-0166-6256>

Seonaid R. Anderson  <https://orcid.org/0000-0001-8556-577X>

Valiyaveetil S. Semeena  <https://orcid.org/0000-0002-1895-449X>

REFERENCES

- Annamalai, H. and Slingo, J.M. (2001) Active/break cycles: diagnosis of the intraseasonal variability of the Asian summer monsoon. *Climate Dynamics*, 18, 85–102.
- Balsamo, G., Albergel, C., Beljaars, A., Boussetta, S., Brun, E., Cloke, H., Dee, D.P., Dutra, E., Muñoz-Sabater, J., Pappenberger, F., de Rosnay, P., Stockdale, T. and Vitart, F. (2015) ERA-Interim/Land: a global land surface reanalysis data set. *Hydrology and Earth System Sciences*, 19, 389–407.
- Barton, E., Taylor, C., Klein, C., Harris, P. and Meng, X. (2021) Observed soil moisture impact on strong convection over mountainous Tibetan Plateau. *Journal of Hydrometeorology*, 22, 561–572.
- Berg, A., Lintner, B., Findell, K. and Giannini, A. (2017) Soil moisture influence on seasonality and large-scale circulation in simulations of the West African monsoon. *Journal of Climate*, 30, 2295–2317.
- Berg, A., Lintner, B.R., Findell, K.L., Malyshev, S., Loikith, P.C. and Gentine, P. (2014) Impact of soil moisture–atmosphere interactions on surface temperature distribution. *Journal of Climate*, 27, 7976–7993.
- Berhane, F., Zaitchik, B. and Badr, H.S. (2015) The Madden–Julian Oscillation’s influence on spring rainy season precipitation over equatorial West Africa. *Journal of Climate*, 28, 8653–8672.
- Bhowmick, M. and Parker, D.J. (2018) Analytical solution to a thermodynamic model for the sensitivity of afternoon deep convective initiation to the surface Bowen ratio. *Quarterly Journal of the Royal Meteorological Society*, 144, 2216–2229.
- Bousquet, E., Mialon, A., Rodriguez-Fernandez, N., Prigent, C., Wagner, F.H. and Kerr, Y.H. (2021) Influence of surface water variations on VOD and biomass estimates from passive microwave sensors. *Remote Sensing of Environment*, 257. <https://doi.org/10.1016/j.rse.2021.112345>.
- Chikoore, H. and Jury, M.R. (2010) Intraseasonal variability of satellite-derived rainfall and vegetation over Southern Africa. *Earth Interact*, 14, 1–26.
- Chug, D. and Dominguez, F. (2019) Isolating the observed influence of vegetation variability on the climate of La Plata river basin. *Journal of Climate*, 32, 4473–4490.
- Cook, K.H. (1999) Generation of the African easterly jet and its role in determining West African precipitation. *Journal of Climate*, 12, 1165–1184.
- C3S (2017). ERA5: Fifth generation of ECMWF atmospheric reanalyses of the global climate. Copernicus Climate Change Service Climate Data Store (CDS).
- Dirmeyer, P.A. (2011) The terrestrial segment of soil moisture–climate coupling. *Geophysical Research Letters*, 38(16). <https://doi.org/10.1029/2011GL048268>.
- Dorigo, W., Wagner, W., Albergel, C., Albrecht, F., Balsamo, G., Brocca, L., Chung, D., Ertl, M., Forkel, M., Gruber, A., Haas, E., Hamer, P.D., Hirschi, M., Ikonen, J., de Jeu, R., Kidd, R., Lahoz, W.A., Liu, Y.Y., Miralles, D., Mistelbauer, T., Nicolai-Shaw, N., Parinussa, R., Pratola, C., Reimer, C., van der Schalie, R., Seneviratne, S.I., Smolander, T. and Lecomte, P. (2017) ESA CCI soil moisture for improved Earth system understanding: state-of-the-art and future directions. *Remote Sensing of Environment*, 203, 185–215.

- Duchon, C.E. (1979) Lanczos filtering in one and two dimensions. *Journal of Applied Meteorology and Climatology*, 18, 1016–1022.
- ECMWF (2016). IFS Documentation – Cy41r2. Part II: Data assimilation. Reading, UK: ECMWF.
- Ferranti, L., Slingo, J.M., Palmer, T.N. and Hoskins, B.J. (1999) The effect of land-surface feedbacks on the monsoon circulation. *Quarterly Journal of the Royal Meteorological Society*, 125, 1527–1550.
- Findell, K.L. and Eltahir, E.A. (2003) Atmospheric controls on soil moisture–boundary layer interactions. Part I: framework development. *Journal of Hydrometeorology*, 4, 552–569.
- Flaounas, E., Janicot, S., Bastin, S., Roca, R. and Mohino, E. (2012) The role of the Indian monsoon onset in the West African monsoon onset: observations and AGCM nudged simulations. *Climate Dynamics*, 38, 965–983.
- Funk, C., Peterson, P., Landsfeld, M., Pedreros, D., Verdin, J., Shukla, S., Husak, G., Rowland, J., Harrison, L., Hoell, A. and Michaelsen, J. (2015) The climate hazards infrared precipitation with stations – a new environmental record for monitoring extremes. *Scientific Data*, 2. <https://doi.org/10.1038/sdata.2015.66>.
- Futyan, J.M. and Del Genio, A.D. (2007) Deep convective system evolution over Africa and the tropical Atlantic. *Journal of Climate*, 20, 5041–5060.
- Gadgil, S. and Asha, G. (1992) Intraseasonal variation of the summer monsoon. I: observational aspects. *Journal of the Meteorological Society of Japan. Series II*, 70, 517–527.
- Gallego-Elvira, B., Taylor, C.M., Harris, P.P., Ghent, D., Veal, K.L. and Folwell, S.S. (2016) Global observational diagnosis of soil moisture control on the land surface energy balance. *Geophysical Research Letters*, 43, 2623–2631.
- Gallego-Elvira, B., Taylor, C.M., Harris, P.P. and Ghent, D. (2019) Evaluation of regional-scale soil moisture–surface flux dynamics in Earth system models based on satellite observations of land surface temperature. *Geophysical Research Letters*, 46, 5480–5488.
- Gruber, A., Dorigo, W.A., Crow, W. and Wagner, W. (2017) Triple collocation-based merging of satellite soil moisture retrievals. *IEEE Transactions on Geoscience and Remote Sensing*, 55, 6780–6792.
- Gruber, A., Scanlon, T., van der Schalie, R., Wagner, W. and Dorigo, W. (2019) Evolution of the ESA CCI soil moisture climate data records and their underlying merging methodology. *Earth System Science Data*, 1–37.
- Gu, G. and Adler, R.F. (2004) Seasonal evolution and variability associated with the West African monsoon system. *Journal of climate*, 17, 3364–3377.
- Guo, Z., Dirmeyer, P.A., Koster, R.D., Sud, Y., Bonan, G., Oleson, K.W., Chan, E., Verseghy, D., Cox, P., Gordon, C.T., McGregor, J.L., Kanae, S., Kowalczyk, E., Lawrence, D., Liu, P., Mocko, D., Lu, C.-H., Mitchell, K., Malyshev, S., McAvaney, B., Oki, T., Yamada, T., Pitman, A., Taylor, C.M., Vasic, R. and Xue, Y. (2006) GLACE: the global land–atmosphere coupling experiment. Part II: analysis. *Journal of Hydrometeorology*, 7, 611–625.
- Hagos, S.M. and Cook, K.H. (2007) Dynamics of the West African monsoon jump. *Journal of Climate*, 20, 5264–5284.
- Hall, N.M., Kiladis, G.N. and Thorncroft, C.D. (2006) Three-dimensional structure and dynamics of African easterly waves. Part II: dynamical modes. *Journal of the Atmospheric Sciences*, 63, 2231–2245.
- Hersbach, H., de Rosnay, P., Bell, B., Schepers, D., Simmons, A., Soci, C., Abdalla, S., Alonso-Balmaseda, M., Balsamo, G., Bechtold, P., Berrisford, P., Bidlot, J.-R., de Boissésion, E., Bonavita, M., Browne, P., Buizza, R., Dahlgren, P., Dee, D.P., Dragani, R., Diamantakis, M., Flemming, J., Forbes, R., Geer, A.J., Haiden, T., Hólm, E.V., Haimberger, L., Hogan, R., Horányi, A., Janiskova, M., Laloyaux, P., Lopez, P., Muñoz-Sabater, J., Peubey, C., Radu, R., Richardson, D., Thépaut, J.-N., Vitart, F., Yang, X., Zsótér, E. and Zuo, H. (2018). Operational global reanalysis: Progress, future directions and synergies with NWP. ERA Report 27, Reading, UK: ECMWF.
- Hersbach, H., Bell, W., Berrisford, P., Horányi, A., Muñoz-Sabatier, J., Nicolas, J., Radu, R., Schepers, D., Simmons, A., Soci, C. and Dee, D.P. (2019) Global reanalysis: Goodbye ERA-Interim, hello ERA5. *ECMWF Newsletter*, 159, 17–24. <https://doi.org/10.21957/vf291hehd7>.
- Hodges, K.I. and Thorncroft, C.D. (1997) Distribution and statistics of African mesoscale convective weather systems based on the ISCCP Meteosat imagery. *Monthly Weather Review*, 125, 2821–2837.
- Hohenegger, C., Brockhaus, P., Bretherton, C.S. and Schär, C. (2009) The soil moisture–precipitation feedback in simulations with explicit and parameterized convection. *Journal of Climate*, 22, 5003–5020.
- Hoinka, K.P. and Castro, M.D. (2003) The Iberian peninsula thermal low. *Quarterly Journal of the Royal Meteorological Society*, 129, 1491–1511.
- Howard, E. and Washington, R. (2018) Characterizing the synoptic expression of the Angola low. *Journal of Climate*, 31, 7147–7165.
- Hsieh, J.-S. and Cook, K.H. (2008) On the instability of the African easterly jet and the generation of African waves: reversals of the potential vorticity gradient. *Journal of the Atmospheric Sciences*, 65, 2130–2151.
- Huffman, G., Bolvin, D., Nelkin, E. and Adler, R. (2016). TRMM (TMPA) precipitation L3 1 day 0.25 degree x 0.25 degree v7, Savtchenko A. (ed.) Greenbelt, MD: Goddard Earth Sciences Data and Information Services Center (GES DISC), DOI 10.5067/TRMM/TMPA/DAY/7, (to appear in print).
- Huffman, G., Stocker, E., Bolvin, D., Nelkin, E. and Jackson, T. (2019). GPM IMERG final precipitation L3 1 day 0.1 degree x 0.1 degree v06, Savtchenko, A. (ed.) Greenbelt, MD: Goddard Earth Sciences Data and Information Services Center (GES DISC), DOI 10.5067/GPM/IMERGDF/DAY/06, (to appear in print).
- Janicot, S. and Sultan, B. (2001) Intra-seasonal modulation of convection in the West African monsoon. *Geophysical Research Letters*, 28, 523–526.
- Janicot, S., Mounier, F., Hall, N.M., Leroux, S., Sultan, B. and Kiladis, G.N. (2009) Dynamics of the West African monsoon. Part IV: analysis of 25–90-day variability of convection and the role of the Indian monsoon. *Journal of Climate*, 22, 1541–1565.
- Janicot, S., Mounier, F., Gervois, S., Sultan, B. and Kiladis, G.N. (2010) The dynamics of the West African monsoon. Part V: the detection and role of the dominant modes of convectively coupled equatorial Rossby waves. *Journal of Climate*, 23, 4005–4024.
- Janicot, S., Caniaux, G., Chauvin, F., De Coëtlogon, G., Fontaine, B., Hall, N., Kiladis, G., Lafore, J.-P., Lavaysse, C., Lavender, S.L., Leroux, S., Marteau, R., Mounier, F., Philippon, N., Roehrig, R., Sultan, B. and Taylor, C.M. (2011) Intraseasonal variability of the West African monsoon. *Atmospheric Science Letters*, 12, 58–66.

- Klein, C. and Taylor, C.M. (2020) Dry soils can intensify mesoscale convective systems. *Proceedings of the National Academy of Sciences USA*, 117, 21132–21137.
- Klein, C., Belušić, D. and Taylor, C.M. (2018) Wavelet scale analysis of mesoscale convective systems for detecting deep convection from infrared imagery. *Journal of Geophysical Research: Atmospheres*, 123, 3035–3050.
- Klein, C., Nkrumah, F., Taylor, C.M. and Adefisan, E.A. (2021) Seasonality and trends of drivers of mesoscale convective systems in southern West Africa. *Journal of Climate*, 34, 71–87.
- Koster, R.D., Sud, Y., Guo, Z., Dirmeyer, P.A., Bonan, G., Oleson, K.W., Chan, E., Verseghy, D., Cox, P., Davies, H., Kowalczyk, E., Gordon, C.T., Kanae, S., Lawrence, D., Liu, P., Mocko, D., Lu, C.-H., Mitchell, K., Malyshev, S., McAvaney, B., Oki, T., Yamada, T., Pitman, A., Taylor, C.M., Vasic, R. and Xue, Y. (2006) GLACE: the global land–atmosphere coupling experiment. Part I: overview. *Journal of Hydrometeorology*, 7, 590–610.
- Koster, R., Schubert, S. and Suarez, M. (2009) Analyzing the concurrence of meteorological droughts and warm periods, with implications for the determination of evaporative regime. *Journal of Climate*, 22, 3331–3341.
- Lafore, J.-P., Flamant, C., Guichard, F., Parker, D., Bouniol, D., Fink, A., Giraud, V., Gosset, M., Hall, N., Höller, H., Jones, S.C., Protat, A., Roca, R., Roux, F., Saïd, F. and Thorncroft, C.D. (2011) Progress in understanding of weather systems in West Africa. *Atmospheric Science Letters*, 12, 7–12.
- Lavaysse, C., Flamant, C., Janicot, S., Parker, D.J., Lafore, J.-P., Sultan, B. and Pelon, J. (2009) Seasonal evolution of the West African heat low: a climatological perspective. *Climate Dynamics*, 33, 313–330.
- Lavender, S.L. and Matthews, A.J. (2009) Response of the West African monsoon to the Madden–Julian Oscillation. *Journal of Climate*, 22, 4097–4116.
- Lavender, S.L., Taylor, C.M. and Matthews, A.J. (2010) Coupled land–atmosphere intraseasonal variability of the West African monsoon in a GCM. *Journal of Climate*, 23, 5557–5571.
- Lawal, K.A., Olaniyan, E., Ishiyaku, I., Hirons, L.C., Thompson, E., Talib, J., Boulton, V.L., Ogungbenro, S.B., Gbode, I.E., Ajayi, V.O., Okogbue, E.C., Adefisan, E.A., Indasi, V.S., Youds, L., Nkikaka, E., Stone, D.A., Nzekwu, R., Folorunso, O., Oyedepo, J.A., New, M.G. and Woolnough, S.J. (2021) Progress and challenges of demand-led co-produced sub-seasonal-to-seasonal (S2S) climate forecasts in Nigeria. *Frontiers in Climate*, 3. <https://doi.org/10.3389/fclim.2021.712502>.
- Leroux, S. and Hall, N.M. (2009) On the relationship between African easterly waves and the African easterly jet. *Journal of the Atmospheric Sciences*, 66, 2303–2316.
- Liebmann, B. and Smith, C.A. (1996) Description of a complete (interpolated) outgoing longwave radiation dataset. *Bulletin of the American Meteorological Society*, 77, 1275–1277.
- Lohou, F., Kergoat, L., Guichard, F., Boone, A., Cappelaere, B., Cohard, J.-M., Demarty, J., Galle, S., Grippa, M., Peugeot, C., Ramier, D., Taylor, C.M. and Timouk, F. (2014) Surface response to rain events throughout the West African monsoon. *Atmospheric Chemistry and Physics*, 14, 3883–3898.
- Madden, R.A. and Julian, P.R. (1994) Observations of the 40–50-day tropical oscillation – a review. *Monthly Weather Review*, 122, 814–837.
- Maloney, E.D. and Shaman, J. (2008) Intraseasonal variability of the West African monsoon and Atlantic ITCZ. *Journal of Climate*, 21, 2898–2918.
- Matthews, A.J. (2004) Intraseasonal variability over tropical Africa during northern summer. *Journal of Climate*, 17, 2427–2440.
- Miralles, D.G., Van Den Berg, M.J., Teuling, A.J. and de Jeu, R.A.M. (2012) Soil moisture–temperature coupling: a multiscale observational analysis. *Geophysical Research Letters*, 39(21). <https://doi.org/10.1029/2012GL053703>.
- Moesinger, L., Dorigo, W., de Jeu, R., van der Schalie, R., Scanlon, T., Teubner, I. and Forkel, M. (2020) The global long-term microwave Vegetation Optical Depth Climate Archive (VODCA). *Earth System Science Data*, 12, 177–196.
- Mohr, K.I. and Thorncroft, C.D. (2006) Intense convective systems in West Africa and their relationship to the African easterly jet. *Quarterly Journal of the Royal Meteorological Society*, 132, 163–176.
- Mounier, F., Janicot, S. and Kiladis, G.N. (2008) The West African monsoon dynamics. Part III: the quasi-biweekly zonal dipole. *Journal of Climate*, 21, 1911–1928.
- Newell, R.E. and Kidson, J.W. (1984) African mean wind changes between Sahelian wet and dry periods. *Journal of Climatology*, 4, 27–33.
- Nicholls, S.D. and Mohr, K.I. (2010) An analysis of the environments of intense convective systems in West Africa in 2003. *Monthly Weather Review*, 138, 3721–3739.
- North, G.R., Bell, T.L., Cahalan, R.F. and Moeng, F.J. (1982) Sampling errors in the estimation of empirical orthogonal functions. *Monthly Weather Review*, 110, 699–706.
- Notaro, M., Wang, F., Yu, Y. and Mao, J. (2020) Projected changes in the terrestrial and oceanic regulators of climate variability across sub-Saharan Africa. *Climate Dynamics*, 55, 1031–1057.
- Parker, D.J., Burton, R., Diongue-Niang, A., Ellis, R., Felton, M., Taylor, C., Thorncroft, C.D., Bessemoulin, P. and Tompkins, A. (2005) The diurnal cycle of the West African monsoon circulation. *Quarterly Journal of the Royal Meteorological Society*, 131, 2839–2860.
- Pegion, K. and Kirtman, B.P. (2008) The impact of air–sea interactions on the simulation of tropical intraseasonal variability. *Journal of Climate*, 21, 6616–6635.
- Peng, J., Loew, A. and Crueger, T. (2017) The relationship between the Madden–Julian Oscillation and the land surface soil moisture. *Remote Sensing of Environment*, 203, 226–239.
- Pielke, R.A.Sr. (2001) Influence of the spatial distribution of vegetation and soils on the prediction of cumulus convective rainfall. *Reviews of Geophysics*, 39, 151–177.
- Pohl, B. and Camberlin, P. (2006) Influence of the Madden–Julian Oscillation on East African rainfall. I: intraseasonal variability and regional dependency. *Quarterly Journal of the Royal Meteorological Society*, 132, 2521–2539.
- Pohl, B., Janicot, S., Fontaine, B. and Marteau, R. (2009) Implication of the Madden–Julian Oscillation in the 40-day variability of the West African monsoon. *Journal of Climate*, 22, 3769–3785.
- Rácz, Z. and Smith, R.K. (1999) The dynamics of heat lows. *Quarterly Journal of the Royal Meteorological Society*, 125, 225–252.
- Rodell, M., Houser, P.R., Jambor, U., Gottschalck, J., Mitchell, K., Meng, C.-J., Arsenault, K., Cosgrove, B., Radakovich, J., Bosilovich, M., Entin, J.K., Walker, J.P., Lohmann, D. and Toll, D. (2004) The global land data assimilation system. *Bulletin of the American Meteorological Society*, 85, 381–394.
- Roehrig, R., Chauvin, F. and Lafore, J.-P. (2011) 10–25-day intraseasonal variability of convection over the Sahel: a role of the Saharan heat low and midlatitudes. *Journal of Climate*, 24, 5863–5878.

- Rowell, D.P. and Milford, J.R. (1993) On the generation of African squall lines. *Journal of Climate*, 6, 1181–1193.
- Russell, J.O., Aiyyer, A., White, J.D. and Hannah, W. (2017) Revisiting the connection between African easterly waves and Atlantic tropical cyclogenesis. *Geophysical Research Letters*, 44, 587–595.
- Saha, S.K., Halder, S., Suryachandra Rao, A. and Goswami, B. (2012) Modulation of ISOs by land–atmosphere feedback and contribution to the interannual variability of Indian summer monsoon. *Journal of Geophysical Research: Atmospheres*, 117(D3). <https://doi.org/10.1029/2011JD017291>.
- Sathyanadh, A., Karipot, A., Ranalkar, M. and Prabhakaran, T. (2016) Evaluation of soil moisture data products over Indian region and analysis of spatio-temporal characteristics with respect to monsoon rainfall. *Journal of Hydrology*, 542, 47–62.
- Schlueter, A., Fink, A.H. and Knippertz, P. (2019a) A systematic comparison of tropical waves over northern Africa. Part II: dynamics and thermodynamics. *Journal of Climate*, 32, 2605–2625.
- Schlueter, A., Fink, A.H., Knippertz, P. and Vogel, P. (2019b) A systematic comparison of tropical waves over northern Africa. Part I: influence on rainfall. *Journal of Climate*, 32, 1501–1523.
- Schroeder, R., McDonald, K.C., Chapman, B.D., Jensen, K., Podest, E., Tessler, Z.D., Bohn, T.J. and Zimmermann, R. (2015) Development and evaluation of a multi-year fractional surface water data set derived from active/passive microwave remote sensing data. *Remote Sensing*, 7, 16688–16732.
- Schwingshackl, C., Hirschi, M. and Seneviratne, S.I. (2017) Quantifying spatiotemporal variations of soil moisture control on surface energy balance and near-surface air temperature. *Journal of Climate*, 30, 7105–7124.
- Senior, C.A., Marsham, J.H., Berthou, S., Burgin, L.E., Folwell, S.S., Kendon, E.J., Klein, C.M., Jones, R.G., Mittal, N., Rowell, D.P., Tomassini, L., Vischel, T., Becker, B., Birch, C.E., Crook, J., Dougill, A.J., Finney, D.L., Graham, R.J., Hart, N.C.G., Jack, C.D., Jackson, L.S., James, R., Koelle, B., Misiani, H., Mwalukanga, B., Parker, D.J., Stratton, R.A., Taylor, C.M., Tucker, S.O., Wainwright, C.M., Washington, R. and Willet, M.R. (2021) Convection-permitting regional climate change simulations for understanding future climate and informing decision-making in Africa. *Bulletin of the American Meteorological Society*, 102, E106–E1223.
- Shekhar, R. and Boos, W.R. (2017) Weakening and shifting of the Saharan shallow meridional circulation during wet years of the West African monsoon. *Journal of Climate*, 30, 7399–7422.
- Sikka, D. and Gadgil, S. (1980) On the maximum cloud zone and the ITCZ over Indian longitudes during the southwest monsoon. *Monthly Weather Review*, 108, 1840–1853.
- Smith, R.K. and Spengler, T. (2011) The dynamics of heat lows over elevated terrain. *Quarterly Journal of the Royal Meteorological Society*, 137, 250–263.
- Sobrinho, J. and Romaguera, M. (2004) Land surface temperature retrieval from MSG1-SEVIRI data. *Remote Sensing of Environment*, 92, 247–254.
- Sossa, A., Liebmann, B., Bladé, I., Allured, D., Hendon, H.H., Peterson, P. and Hoell, A. (2017) Statistical connection between the Madden–Julian Oscillation and large daily precipitation events in West Africa. *Journal of Climate*, 30, 1999–2010.
- Srinivasan, J., Gadgil, S. and Webster, P. (1993) Meridional propagation of large-scale monsoon convective zones. *Meteorology and Atmospheric Physics*, 52, 15–35.
- Sultan, B. and Janicot, S. (2000) Abrupt shift of the ITCZ over West Africa and intra-seasonal variability. *Geophysical Research Letters*, 27, 3353–3356.
- Sultan, B. and Janicot, S. (2003) The West African monsoon dynamics. Part II: the “pre-onset” and “onset” of the summer monsoon. *Journal of Climate*, 16, 3407–3427.
- Sultan, B., Baron, C., Dingkuhn, M., Sarr, B. and Janicot, S. (2005) Agricultural impacts of large-scale variability of the West African monsoon. *Agricultural and Forest Meteorology*, 128, 93–110.
- Talib, J., Taylor, C.M., Duan, A. and Turner, A.G. (2021) Intraseasonal soil moisture–atmosphere feedbacks on the Tibetan Plateau circulation. *Journal of Climate*, 34, 1789–1807.
- Taylor, C.M. (2008) Intraseasonal land–atmosphere coupling in the West African monsoon. *Journal of Climate*, 21, 6636–6648.
- Taylor, C.M. (2015) Detecting soil moisture impacts on convective initiation in Europe. *Geophysical Research Letters*, 42, 4631–4638.
- Taylor, C.M., Parker, D.J. and Harris, P.P. (2007) An observational case study of mesoscale atmospheric circulations induced by soil moisture. *Geophysical Research Letters*, 34(15). <https://doi.org/10.1029/2007GL030572>.
- Taylor, C.M., Parker, D.J., Kalthoff, N., Gaertner, M.A., Philippon, N., Bastin, S., Harris, P.P., Boone, A., Guichard, F., Agusti-Panareda, A., Baldi, M., Cerlini, P., Descroix, L., Douville, H., Flamant, C., Grandpeix, J.-Y. and Polcher, J. (2011) New perspectives on land–atmosphere feedbacks from the African Monsoon Multidisciplinary Analysis. *Atmospheric Science Letters*, 12(1), 38–44.
- Taylor, C.M., de Jeu, R.A., Guichard, F., Harris, P.P. and Dorigo, W.A. (2012) Afternoon rain more likely over drier soils. *Nature*, 489, 423–426.
- Taylor, C.M., Birch, C.E., Parker, D.J., Dixon, N., Guichard, F., Nikulin, G. and Lister, G.M. (2013) Modeling soil moisture–precipitation feedback in the Sahel: importance of spatial scale versus convective parameterization. *Geophysical Research Letters*, 40, 6213–6218.
- Teuling, A., Seneviratne, S.I., Williams, C. and Troch, P.A. (2006) Observed timescales of evapotranspiration response to soil moisture. *Geophysical Research Letters*, 33(23). <https://doi.org/10.1029/2006GL028178>.
- Thorncroft, C.D. and Blackburn, M. (1999) Maintenance of the African easterly jet. *Quarterly Journal of the Royal Meteorological Society*, 125, 763–786.
- Thorncroft, C.D. and Hodges, K. (2001) African easterly wave variability and its relationship to Atlantic tropical cyclone activity. *Journal of Climate*, 14, 1166–1179.
- Thorncroft, C.D., Hall, N.M. and Kiladis, G.N. (2008) Three-dimensional structure and dynamics of African easterly waves. Part III: genesis. *Journal of Atmospheric Sciences*, 65, 3596–3607.
- Timouk, F., Kergoat, L., Mougou, E., Lloyd, C., Ceschia, E., Cohard, J.-M., De Rosnay, P., Hiernaux, P., Demarez, V. and Taylor, C. (2009) Response of surface energy balance to water regime and vegetation development in a Sahelian landscape. *Journal of Hydrology*, 375, 178–189.
- Ulaby, F.T., Moore, R.K. and Fung, A.K. (1982) *Microwave Remote Sensing – Active and Passive, vol II, Radar Remote Sensing and Surface Scattering and Emission Theory*. Norwood, MA: Artech House.
- Unnikrishnan, C., Rajeevan, M. and Rao, S.V.B. (2017) A study on the role of land–atmosphere coupling on the South Asian monsoon

- climate variability using a regional climate model. *Theoretical and Applied Climatology*, 127, 949–964.
- van der Schalie, R., Preimesberger, W., Pasik, A., Scanlon, T. and Kidd, R. (2020). ESA Climate Change Initiative plus soil moisture. Product user guide (PUG).
- Ventrice, M.J., Thorncroft, C.D. and Roundy, P.E. (2011) The Madden–Julian Oscillation’s influence on African easterly waves and downstream tropical cyclogenesis. *Monthly Weather Review*, 139, 2704–2722.
- Vizy, E.K. and Cook, K.H. (2018) Mesoscale convective systems and nocturnal rainfall over the West African Sahel: role of the inter-tropical front. *Climate Dynamics*, 50, 587–614.
- Wagner, W., Hahn, S., Kidd, R., Melzer, T., Bartalis, Z., Hasenauer, S., Figa-Saldaña, J., De Rosnay, P., Jann, A., Schneider, S., Komma, J., Kubu, G., Brugger, K., Aubrecht, C., Züger, J., Gangkofner, U., Kienberger, S., Brocca, L., Wang, Y., Blöschl, G., Eitzinger, J. and Steinnocher, K. (2013) The ASCAT soil moisture product: a review of its specifications, validation results, and emerging applications. *Meteorologische Zeitschrift*, 22, 5–33.
- Waliser, D.E. (2006). Intraseasonal variability, pp.203–257 in *The Asian Monsoon*, Wang, B. (ed.) Berlin: Springer Praxis.
- Wang, J., Wang, W., Fu, X. and Seo, K.-H. (2012) Tropical intraseasonal rainfall variability in the CFSR. *Climate Dynamics*, 38, 2191–2207.
- Webster, P.J. (1983) Mechanisms of monsoon low-frequency variability: surface hydrological effects. *Journal of Atmospheric Sciences*, 40, 2110–2124.
- Yu, Y., Notaro, M., Wang, F., Mao, J., Shi, X. and Wei, Y. (2017) Observed positive vegetation–rainfall feedbacks in the Sahel dominated by a moisture recycling mechanism. *Nature Communications*, 8, 1–9.

How to cite this article: Talib, J., Taylor, C.M., Klein, C., Harris, B.L., Anderson, S.R. & Semeena, V.S. (2022) The sensitivity of the West African monsoon circulation to intraseasonal soil moisture feedbacks. *Quarterly Journal of the Royal Meteorological Society*, 148(745), 1709–1730. Available from: <https://doi.org/10.1002/qj.4274>